Chapter 5

Effective Properties of Long-fiber Piezoelectric Composites

5.1 Introduction

Recently, piezoelectric materials have gained a huge attraction in the field of smart materials due to their sensing and actuating capabilities. These materials have an excellent property of converting energy from a mechanical to an electrical domain and vice-versa. This property of reciprocity in the energy conversions makes them a wonderful class of materials to have many advanced applications in structural health monitoring, vibration and noise control, ultrasonic imaging, aeroelastic control, underwater applications etc. Despite significant improvements made in fabrication of piezoelectric materials so as to enhance their electromechanical coupling characteristics, the use of monolithic material has certain limitations such as brittleness, difficulty to attach with the curved surfaces and limited range of coupled properties. When bonded with or embedded in flexible structures, these materials provide structures having excellent self-monitoring and self-controlling capabilities. The tailoring of material properties, i.e., the effective elastic, piezoelectric and dielectric coefficients could provide structures having more stability and efficiency.

In recent years, numerous analytical and numerical models have been developed for understanding the electromechanical properties of piezoelectric composites under different fiber volume fractions. Newnham *et. al.* in [7] developed an analytical model based on series and parallel connectivity for piezoelectric and pyroelectric structure-property relations. Shaktivel *et. al.* [130] also adopted a similar model to evaluate effective thermo-electro-elastic properties of 1-3 piezoelectric composites. Based on a

modified cube approach, Banno [19] developed an analytical model to evaluate effective coefficients of piezoelectric ceramics with closed (0-3) and open (1-3) pores. Mallik *et. al.* [131] derived effective properties of piezoelectric fiber-reinforced composites (PFRC) with the help of two micromechanics methods viz. strength of materials (SM) approach and methods of cells (MOC). Piezoelectric fibers are oriented longitudinally in the matrix and the electric field is applied in the direction transverse to the fiber direction. The study predicted improved piezoelectric properties to a transverse direction to that of the applied electric field. Later, Kumar *et. al.* [132] studied the effects of thermal fields on the overall effective coefficients of the piezoelectric fiber reinforced composites using the strength of materials (SM) approach. A micromechanics model based on method of cells (MOC) is developed to predict the effective coefficients of piezoelectric fiber-reinforced composites considering different electric fields in the fiber and matrix by [133]. His prediction for the piezoelectric constant, which gives rise to actuation in the fiber direction, does not show improvement over that of the piezoelectric material alone. Smith *et. al.* [102] used strength of materials approach to predict effective properties of 1-3 piezoelectric composites. The construct of such composites are the rods of piezoelectric materials embedded vertically, i.e., aligned along the thickness of the composite in a polymer-based matrix such that the electric fields are applied along the length of the piezoelectric fibers. These composites show marginal improvement of the effective piezoelectric constant of the piezoelectric composite, which quantifies the deformations in the fiber direction. Dunn *et. al.* [32] evaluated the effective properties of multiphase composites through dilute, self-consistent and Mori-Tanaka approximations. The effective properties of a short fiber inclusion problem are derived through the Eshelby tensor method by several researchers [23,27]. The equivalent inclusion method is applied to study the work hardening behaviour of piezoelectric composites by [93]. The effective

properties of platelets reinforced piezoelectric composite was investigated by [134] with self-consistent and Mori-Tanaka methods.

Several numerical models based on unit cell or representative volume element (RVE) have also been developed to understand the constitutive behaviour of 1-3 piezoelectric composites. Pettermann *et. al.* [73] investigated electro-elastic behaviour of piezoelectric composites with periodic arrangements of continuous aligned fibers using the unit-cell model. In [135], Berger *et. al.* presented a finite element approach based on RVE to predict the overall effective coefficients of periodic transversely isotropic piezoelectric fiber composites. Poizat *et. al.* [60] developed a finite element model based on unit-cell approach to determine overall effective electro-elastic coefficients for 0-3 and 1-3 piezoelectric composites as a function of fiber volume fraction and fiber's aspect ratio. In [136], Bennett *et. al.* developed a finite element model for thickness mode operations of 1-3 piezocomposite used commonly in hydrophone operations. This paper also studied the effects of the lateral pressures on such composites that typically occur in a hydrostatic environment. Kar-Gupta *et. al.* [83] studied the effect of poling characteristics of fiber and matrix phases on the overall electromechanical behaviour of a 1-3 piezocomposite adopting a finite element based numerical model. In [137], a model based on finite element method to study the effects of debonding in the fiber matrix interface on the overall effective properties is developed.

Shaktivel *et. al.* [130,138,139] have effectively used the parallel and series slab model based on strength of materials approach to evaluate the performance parameters of 1-3-2 piezoelectric composites where both fiber and matrix materials are piezoelectric active. A parametric study has been conducted to investigate the effects of poling characteristics of fiber phases on the overall properties of piezocomposites. The performance parameters have also been evaluated in terms of figure of merits to study the

characteristics of piezocomposites as transducers for underwater acoustics and biomedical imaging applications. The results showed that the predicted variations in effective elastic, piezoelectric and dielectric material constants as a function of fiber volume fraction are nonlinear in nature.

The majority of the literature which studies the effective coefficients of piezoelectric inclusion and piezoelectric fiber reinforced composites follows Eshelby tensor approach, strength of materials approach, method of cells, shear lag method or finite element method. In the present paper, the authors have studied the effective properties through modified strength of materials and energy-based approach. The mathematical models have been developed through these approaches to investigate the effects of fiber geometry and orientation on overall effective properties of a piezoelectric composites. The overall effective properties, i.e., elastic, piezoelectric and dielectric coefficients are derived in form of expressions as a function of fiber volume fraction. The theoretical results hence derived are compared with the strength of materials (SM) approach discussed in the literature [131,132].

5.2 Constitutive Relations

The constitutive relations for the material of piezoelectric medium in double index notation as given in [140] are

$$\sigma_{ij} = C^{E}_{ijkl}\epsilon_{kl} - e_{mij}E_m \tag{5.1a}$$

$$D_n = e^{T}_{nkl}\epsilon_{kl} + \kappa^{\epsilon}_{nm}E_m \tag{5.1b}$$

where, σ is the stress tensor, ϵ is the strain tensor, E is the electric field vector, D is the dielectric displacement vector, C is the stiffness matrix, e is the piezoelectric stress coefficient matrix, κ is the dielectric constant matrix and i, j, k, l, m are indices representing the field quantities and material constants. It should be observed that the

stress and strain are represented using two index notations whereas the electric field and dielectric displacement are represented using single index notation since electric field can be applied only in normal directions. Thus, all these indices take values from 1 to 3. Superscript E stands for property at constant electric field, superscript ϵ stands for property at constant strain and superscript T stands for the transpose of matrix. The constitutive relations shown in Eqn. (5.1a) and (5.1b) can be represented in the matrix form as

$$\begin{Bmatrix}\sigma_{11}\\ \sigma_{22}\\ \sigma_{33}\\ \sigma_{23}\\ \sigma_{31}\\ \sigma_{12}\end{Bmatrix} = \begin{bmatrix} C^E_{1111} & C^E_{1122} & C^E_{1133} & C^E_{1123} & C^E_{1131} & C^E_{1112}\\ C^E_{2211} & C^E_{2222} & C^E_{2233} & C^E_{2223} & C^E_{2231} & C^E_{2212}\\ C^E_{3311} & C^E_{3322} & C^E_{3333} & C^E_{3323} & C^E_{3331} & C^E_{3312}\\ C^E_{2311} & C^E_{2322} & C^E_{2333} & C^E_{2323} & C^E_{2331} & C^E_{2312}\\ C^E_{3111} & C^E_{3122} & C^E_{3133} & C^E_{3123} & C^E_{3131} & C^E_{3112}\\ C^E_{1211} & C^E_{1222} & C^E_{1233} & C^E_{1223} & C^E_{1231} & C^E_{1212}\end{bmatrix}\begin{Bmatrix}\epsilon_{11}\\ \epsilon_{22}\\ \epsilon_{33}\\ \epsilon_{23}\\ \epsilon_{31}\\ \epsilon_{12}\end{Bmatrix} - \begin{bmatrix} e_{111} & e_{211} & e_{311}\\ e_{122} & e_{222} & e_{322}\\ e_{133} & e_{233} & e_{333}\\ e_{123} & e_{223} & e_{323}\\ e_{131} & e_{231} & e_{331}\\ e_{112} & e_{212} & e_{312}\end{bmatrix}\begin{Bmatrix}E_1\\ E_2\\ E_3\end{Bmatrix} \tag{5.2a}$$

$$\begin{Bmatrix}D_1\\ D_2\\ D_3\end{Bmatrix} = \begin{bmatrix} e_{111} & e_{122} & e_{133} & e_{123} & e_{131} & e_{112}\\ e_{211} & e_{222} & e_{233} & e_{223} & e_{231} & e_{212}\\ e_{311} & e_{322} & e_{333} & e_{323} & e_{331} & e_{312}\end{bmatrix}\begin{Bmatrix}\epsilon_{11}\\ \epsilon_{22}\\ \epsilon_{33}\\ \epsilon_{23}\\ \epsilon_{31}\\ \epsilon_{12}\end{Bmatrix} + \begin{bmatrix} \kappa^{\epsilon}_{11} & 0 & 0\\ 0 & \kappa^{\epsilon}_{22} & 0\\ 0 & 0 & \kappa^{\epsilon}_{33}\end{bmatrix}\begin{Bmatrix}E_1\\ E_2\\ E_3\end{Bmatrix} \tag{5.2b}$$

For convenience, stress and strain components can also be represented in single index notation as, 11→1, 22→2, 33→3, 23→4, 31→5, 12→6. Now, the constitutive equations shown in Eqn. (5.1a) and (5.1b) can be represented as

$$\sigma_i = C^E_{ij}\epsilon_j - e_{ik}E_k \tag{5.3a}$$

$$D_k = e_{kj}^T \epsilon_j + \kappa_{km}^{\epsilon} E_m \tag{5.3b}$$

where the indices i and j varies from 1 to 6 and indices k and m varies from 1 to 3. The matrix representation of Eqn. (5.3a) and (5.3b) can be written as

$$\begin{Bmatrix} \sigma_1 \\ \sigma_2 \\ \sigma_3 \\ \sigma_4 \\ \sigma_5 \\ \sigma_6 \end{Bmatrix} = \begin{bmatrix} C_{11}^E & C_{12}^E & C_{13}^E & C_{14}^E & C_{15}^E & C_{16}^E \\ C_{21}^E & C_{22}^E & C_{23}^E & C_{24}^E & C_{25}^E & C_{26}^E \\ C_{31}^E & C_{32}^E & C_{33}^E & C_{34}^E & C_{35}^E & C_{36}^E \\ C_{41}^E & C_{42}^E & C_{43}^E & C_{44}^E & C_{45}^E & C_{46}^E \\ C_{51}^E & C_{52}^E & C_{53}^E & C_{54}^E & C_{55}^E & C_{56}^E \\ C_{61}^E & C_{62}^E & C_{63}^E & C_{64}^E & C_{65}^E & C_{66}^E \end{bmatrix} \begin{Bmatrix} \epsilon_1 \\ \epsilon_2 \\ \epsilon_3 \\ \epsilon_4 \\ \epsilon_5 \\ \epsilon_6 \end{Bmatrix} - \begin{bmatrix} e_{11} & e_{21} & e_{31} \\ e_{12} & e_{22} & e_{32} \\ e_{13} & e_{23} & e_{33} \\ e_{14} & e_{24} & e_{34} \\ e_{15} & e_{25} & e_{35} \\ e_{16} & e_{26} & e_{36} \end{bmatrix} \begin{Bmatrix} E_1 \\ E_2 \\ E_3 \end{Bmatrix} \tag{5.4a}$$

$$\begin{Bmatrix} D_1 \\ D_2 \\ D_3 \end{Bmatrix} = \begin{bmatrix} e_{11} & e_{12} & e_{13} & e_{14} & e_{15} & e_{16} \\ e_{21} & e_{22} & e_{23} & e_{24} & e_{25} & e_{26} \\ e_{31} & e_{32} & e_{33} & e_{34} & e_{35} & e_{36} \end{bmatrix} \begin{Bmatrix} \epsilon_1 \\ \epsilon_2 \\ \epsilon_3 \\ \epsilon_4 \\ \epsilon_5 \\ \epsilon_6 \end{Bmatrix} + \begin{bmatrix} \kappa_{11}^{\epsilon} & 0 & 0 \\ 0 & \kappa_{22}^{\epsilon} & 0 \\ 0 & 0 & \kappa_{33}^{\epsilon} \end{bmatrix} \begin{Bmatrix} E_1 \\ E_2 \\ E_3 \end{Bmatrix} \tag{5.4b}$$

For the current analysis piezoelectric fiber is transversely isotropic and the matrix is isotropic. Thus elastic, piezoelectric and dielectric matrices of the piezoelectric fiber can be represented as

$$[\boldsymbol{C}] = \begin{bmatrix} C_{11}^{fE} & C_{12}^{fE} & C_{13}^{fE} & 0 & 0 & 0 \\ C_{21}^{fE} & C_{22}^{fE} & C_{23}^{fE} & 0 & 0 & 0 \\ C_{31}^{fE} & C_{32}^{fE} & C_{33}^{fE} & 0 & 0 & 0 \\ 0 & 0 & 0 & C_{44}^{fE} & 0 & 0 \\ 0 & 0 & 0 & 0 & C_{55}^{fE} & 0 \\ 0 & 0 & 0 & 0 & 0 & C_{66}^{fE} \end{bmatrix}, [\boldsymbol{e}] = \begin{bmatrix} 0 & 0 & e_{31}^{f} \\ 0 & 0 & e_{32}^{f} \\ 0 & 0 & e_{33}^{f} \\ 0 & e_{24}^{f} & 0 \\ e_{15}^{f} & 0 & 0 \\ 0 & 0 & 0 \end{bmatrix}, \quad (5.5a)$$

$$[\boldsymbol{\kappa}] = \begin{bmatrix} \kappa_{11}^{f\epsilon} & 0 & 0 \\ 0 & \kappa_{22}^{f\epsilon} & 0 \\ 0 & 0 & \kappa_{33}^{f\epsilon} \end{bmatrix}$$

and for the matrix medium the elastic and dielectric matrices is given as

$$[\boldsymbol{C}] = \begin{bmatrix} C_{11}^{mE} & C_{12}^{mE} & C_{13}^{mE} & 0 & 0 & 0 \\ C_{21}^{mE} & C_{22}^{mE} & C_{23}^{mE} & 0 & 0 & 0 \\ C_{31}^{mE} & C_{32}^{mE} & C_{33}^{mE} & 0 & 0 & 0 \\ 0 & 0 & 0 & C_{44}^{mE} & 0 & 0 \\ 0 & 0 & 0 & 0 & C_{55}^{mE} & 0 \\ 0 & 0 & 0 & 0 & 0 & C_{66}^{mE} \end{bmatrix}, [\boldsymbol{\kappa}] = \begin{bmatrix} \kappa_{11}^{m\epsilon} & 0 & 0 \\ 0 & \kappa_{22}^{m\epsilon} & 0 \\ 0 & 0 & \kappa_{33}^{m\epsilon} \end{bmatrix} \quad (5.5b)$$

Further, with the consideration of all the conditions mentioned above the constitutive relations for fiber can be written in form of equations from Eqns. (5.6a) to (5.6i) as

$$\sigma_1^f = C_{11}^{fE}\epsilon_1^f + C_{12}^{fE}\epsilon_2^f + C_{13}^{fE}\epsilon_3^f - e_{31}^f E_3^f \quad (5.6a)$$

$$\sigma_2^f = C_{12}^{fE}\epsilon_1^f + C_{22}^{fE}\epsilon_2^f + C_{23}^{fE}\epsilon_3^f - e_{32}^f E_3^f \quad (5.6b)$$

$$\sigma_3^f = C_{13}^{fE}\epsilon_1^f + C_{23}^{fE}\epsilon_2^f + C_{33}^{fE}\epsilon_3^f - e_{33}^f E_3^f \quad (5.6c)$$

$$\sigma_4^f = C_{44}^{fE}\epsilon_4^f - e_{24}^f E_2^f \quad (5.6d)$$

$$\sigma_5^f = C_{55}^{fE}\epsilon_5^f - e_{15}^f E_1^f \quad (5.6e)$$

$$\sigma_6^f = C_{66}^{fE}\epsilon_6^f \quad (5.6f)$$

$$D_1^f = e_{15}^{fE}\epsilon_5^f + \kappa_{11}^{f\epsilon}E_1^f \quad (5.6g)$$

$$D_2^f = e_{24}^{fE}\epsilon_4^f + \kappa_{22}^{f\epsilon}E_2^f \quad (5.6h)$$

$$D_3^f = e_{31}^{fE}\epsilon_1^f + e_{32}^{fE}\epsilon_2^f + e_{33}^{fE}\epsilon_3^f + \kappa_{33}^{f\epsilon}E_3^f \quad (5.6i)$$

Similarly, the constitutive relations for matrices can be written in the form of equations from Eqns. (5.7a) to (5.7i) as

$$\sigma_1^m = C_{11}^{mE}\epsilon_1^m + C_{12}^{mE}\epsilon_2^m + C_{13}^{mE}\epsilon_3^m \quad (5.7a)$$

$$\sigma_2^m = C_{12}^{mE}\epsilon_1^m + C_{22}^{mE}\epsilon_2^m + C_{23}^{mE}\epsilon_3^m \quad (5.7b)$$

$$\sigma_3^m = C_{13}^{mE}\epsilon_1^m + C_{23}^{mE}\epsilon_2^m + C_{33}^{mE}\epsilon_3^m \quad (5.7c))$$

$$\sigma_4^m = C_{44}^{mE}\epsilon_4^m \quad (5.7d))$$

$$\sigma_5^m = C_{55}^{mE}\epsilon_5^m \quad (5.7e))$$

$$\sigma_6^m = C_{66}^{mE}\epsilon_6^m \quad (5.7f)$$

$$D_1^m = \kappa_{11}^{m\epsilon}E_1^m \quad (5.7g))$$

$$D_2^m = e_{24}^{mE}\epsilon_4^m + \kappa_{22}^{m\epsilon}E_2^m \quad (5.7h))$$

$$D_3^m = e_{31}^{mE}\epsilon_1^m + e_{32}^{mE}\epsilon_2^m + e_{33}^{mE}\epsilon_3^m + \kappa_{33}^{m\epsilon}E_3^m \quad (5.7i))$$

The superscript *f* and *m* denote the material properties of the fiber and the matrix respectively.

5.3 Micromechanics Model

5.3.1 Modified Strength of Materials Method (MSM Model)

Piezoelectric fiber reinforced composites consist of a series of long piezoelectric fibers embedded in a matrix material. The bulk PFRC can be visualized as an assembly of rectangular representative volume elements (RVE) that contains both fiber and matrix materials. Figure 5.1 shows a square array of fibers of an arbitrary cross-section and Figure 5.2 gives a representative volume element (RVE) of such an array. Micromechanics model developed on the basis of MSM and energy method is confined to such an element containing both fiber and matrix materials. However, in an average

sense the effective properties derived from such an RVE would be the same as that of the bulk material. The validity of the present model requires certain assumptions.

Assumptions:

i. The proposed composite is homogeneous in construction.
ii. Fibers are continuous and parallel.
iii. The fiber and matrix materials are linearly elastic.
iv. There is a perfect bonding along the fiber-matrix interface throughout the domain.
v. Fibers are piezoelectrically active whereas matrix is piezoelectrically passive.
vi. The composite is subjected to a constant electric field in the direction transverse to the fiber direction, and the electric field is assumed to be the same for both phases (the fiber and matrix).
vii. In the linear constitutive equations of any piezoelectric material, the elastic and piezoelectric coefficients are defined at a constant electric field and the dielectric constants are defined at a constant strain.

Piezoelectric fiber reinforced composites consist of piezoelectric fibers embedded in a matrix material. The bulk PFRC can be visualized as an assembly of rectangular representative volume elements (RVE) that contains both fiber and matrix phases. Figure 5.1 (a) shows a square array of circular fibers embedded in soft matrix materials and Figure 5.1 (b) illustrates a representative volume element (RVE) of such an array. The circular cross-section of fiber is converted into a square of equivalent area and the RVE is divided into subregions as shown in Figure 5.2.

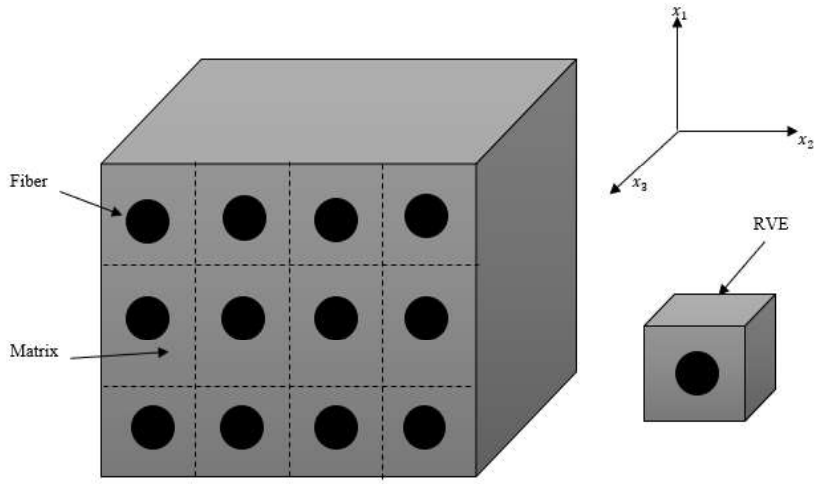

Figure 5.1 (a) Schematic of a piezoelectric fiber reinforced composite PFRC (1-3 piezocomposite).

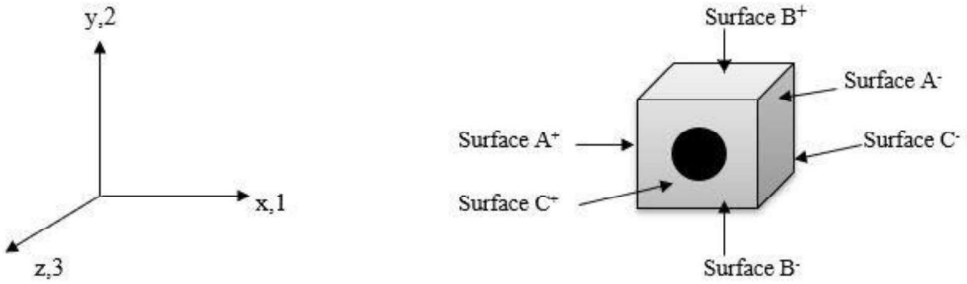

Figure 5.1 (b) A representative volume element (RVE).

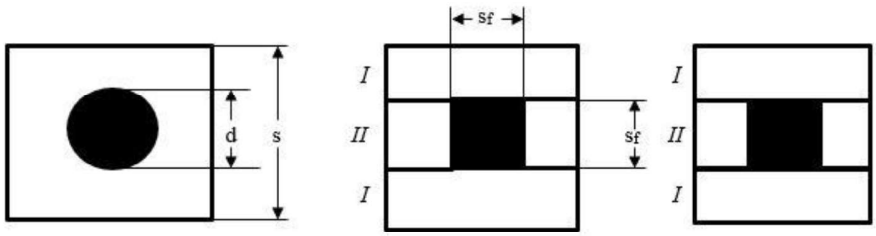

Figure 5.2 Transverse cross-section of a representative volume element of PFRC (1-3 piezocomposite).

The circular cross-section of fiber is converted into a square with equivalent area and the RVE is further divided into subregions as shown in Figure 5.2. The cross-sectional area a_f of an arbitrary shape fiber can be modified into an equivalent cross-sectional area of a square shape fiber having side length s_f. Since the length of side of the RVE is s, the cross-sectional area of the RVE becomes s^2. As mentioned above the cross-sectional area of arbitrary shape fiber is modified into the equivalent area of a square shape fiber, it can be expressed as

$$s_f^2 = a_f \text{ or } s_f = \sqrt{a_f} \tag{5.8}$$

Fiber volume fraction for longitudinal fiber reinforced composite is the ratio of cross-sectional area of the fiber to the total cross-sectional area of the RVE, and can be written as

$$v_f = \frac{a_f}{s^2} = \frac{s_f^2}{s^2} \tag{5.9}$$

or,

$$\frac{s_f}{s} = \sqrt{v_f} \tag{5.10}$$

As it can be observed from Figure 5.2, the matrix dimension is $s_m = s - s_f$, and from Eqn. (5.10) it can be written as

$$\frac{s_m}{s} = 1 - \sqrt{v_f} \tag{5.11}$$

Figure 5.2 illustrates that the RVE can be divided into sub-regions I and II, sub-region I is matrix dominated while II is a composite consisting of both fiber and matrix phases. In the present micromechanics approach, first the problem is modeled to compute the effective properties of sub region II as a series connection of fiber and matrix subjected to transverse normal stress followed by the calculation of overall effective properties taking sub region I and II as parallel connection subjected to transverse normal stress.

Considering series connection of fiber and matrix in sub region II subjected to transverse loading, geometric compatibility requires

$$\delta_{22}^{II} = \delta_{22}^{IIf} + \delta_{22}^{IIm} \tag{5.12}$$

δ_{22}^{IIf}, δ_{22}^{IIm} are displacements in the fiber and matrix when transverse loading in direction-2 is applied. Consequently,

$$\epsilon_{22}^{II} s = \epsilon_{22}^{f} s_f + \epsilon_{22}^{m} s_m \tag{5.13}$$

Using Eqns. (5.10) and (5.11), Eqn. (5.13) can be written as

$$\epsilon_{22}^{II} = \sqrt{v_f}\epsilon_{22}^{f} + (1 - \sqrt{v_f})\epsilon_{22}^{m} \tag{5.14}$$

Similarly, for direction-3, the relation can be written as

$$\epsilon_{33}^{II} = \sqrt{v_f}\epsilon_{33}^{f} + (1 - \sqrt{v_f})\epsilon_{33}^{m} \tag{5.15}$$

As bonding between fiber and matrix interface is assumed to be perfect, therefore the strains are same in direction-1

$$\epsilon_{11}^{II} = \epsilon_{11}^{f} = \epsilon_{11}^{m} \tag{5.16}$$

Also, there is an electric field applied in transverse direction that is same for both the fiber and the matrix in sub region II

$$E_3^{II} = E_3^f = E_3^m \tag{5.17}$$

Since, stresses in fiber and matrix phases in transverse directions-2 and 3 are equal, it can be represented as

$$\sigma_{22}^f = \sigma_{22}^m \tag{5.18}$$

$$\sigma_{33}^f = \sigma_{33}^m \tag{5.19}$$

Using Eqns. (5.6b), (5.7b), (5.14), (5.15), (5.16), and (5.17) into Eqns. (5.18) and (5.6c), (5.7c), (5.14), (5.15), (5.16) and (5.17) into Eqn. (5.19), the following relations are obtained

$$A_1\epsilon_{22}^f + A_2\epsilon_{33}^f = B_1\epsilon_{11}^c + B_2\epsilon_{22}^c + B_3\epsilon_{33}^c - B_4E_3^c \tag{5.20}$$

$$A_2\epsilon_{22}^f + A_3\epsilon_{33}^f = B_5\epsilon_{11}^c + B_3\epsilon_{22}^c + B_6\epsilon_{33}^c - B_7E_3^c \tag{5.21}$$

where,

$$A_1 = \left(1 - \sqrt{v_f}\right)C_{22}^{fE} + \sqrt{v_f}C_{22}^{mE} \tag{5.22}$$

$$A_2 = \left(1 - \sqrt{v_f}\right)C_{23}^{fE} + \sqrt{v_f}C_{23}^{mE} \tag{5.23}$$

$$A_3 = \left(1 - \sqrt{v_f}\right)C_{33}^{fE} + \sqrt{v_f}C_{33}^{mE} \tag{5.24}$$

$$B_1 = \left(1 - \sqrt{v_f}\right)(C_{12}^{mE} - C_{12}^{fE}) \tag{5.25}$$

$$B_2 = C_{22}^{mE} \tag{5.26}$$

$$B_3 = C_{23}^{mE} \tag{5.27}$$

$$B_4 = \left(1 - \sqrt{v_f}\right)(e_{32}^m - e_{32}^f) \tag{5.28}$$

$$B_5 = \left(1 - \sqrt{v_f}\right)(C_{13}^{mE} - C_{13}^{fE}) \tag{5.29}$$

$$B_6 = C_{33}^{mE} \tag{5.30}$$

$$B_7 = \left(1 - \sqrt{v_f}\right)(e_{33}^{m} - e_{33}^{f}) \tag{5.31}$$

On solving Eqns. (5.18) and (5.19), the following equations are obtained

$$\epsilon_{22}^{f} = F_1\epsilon_{11}^{c} + F_2\epsilon_{22}^{c} + F_3\epsilon_{33}^{c} - F_4E_3^{c} \tag{5.32}$$

$$\epsilon_{33}^{f} = G_1\epsilon_{11}^{c} + G_2\epsilon_{22}^{c} + G_3\epsilon_{33}^{c} - G_4E_3^{c} \tag{5.33}$$

where,

$$G_1 = \frac{A_2B_1 - A_1B_5}{A_2^2 - A_1A_3} \tag{5.34}$$

$$G_2 = \frac{A_2B_2 - A_1B_3}{A_2^2 - A_1A_3} \tag{5.35}$$

$$G_3 = \frac{A_2B_3 - A_1B_6}{A_2^2 - A_1A_3} \tag{5.36}$$

$$G_4 = \frac{AB_4 - A_1B_7}{A_2^2 - A_1A_3} \tag{5.37}$$

$$F_1 = \frac{B_1 - A_2G_1}{A_1} \tag{5.38}$$

$$F_2 = \frac{B_2 - A_2G_2}{A_1} \tag{5.39}$$

$$F_3 = \frac{B_3 - A_2G_3}{A_1} \tag{5.40}$$

$$F_4 = \frac{B_4 - A_2G_4}{A_1} \tag{5.41}$$

Using Eqns. (5.4a), (5.4b), (5.14), (5.15), (5.16), (5.17) into Eqns. (5.21) and (5.32) transverse stresses in direction-2 can be expressed as

$$\sigma_{22}^{f} = I_1\epsilon_{11}^{c} + I_2\epsilon_{22}^{c} + I_3\epsilon_{33}^{c} - I_4E_3^{c} \tag{5.42}$$

$$\sigma_{22}^{m} = J_1\epsilon_{11}^{c} + J_2\epsilon_{22}^{c} + J_3\epsilon_{33}^{c} - J_4 E_3^{c} \tag{5.43}$$

where,

$$I_1 = C_{12}^{fE} + C_{22}^{fE}F_1 + C_{23}^{fE}G_1 \tag{5.44}$$

$$I_2 = C_{22}^{fE}F_2 + C_{23}^{fE}G_2 \tag{5.45}$$

$$I_3 = C_{22}^{fE}F_3 + C_{23}^{fE}G_3 \tag{5.46}$$

$$I_4 = C_{22}^{fE}F_4 + C_{23}^{fE}G_4 \tag{5.47}$$

and,

$$J_1 = C_{12}^{mE} + \frac{\sqrt{v_f}C_{22}^{mE}}{1-\sqrt{v_f}}F_1 - \frac{\sqrt{v_f}C_{23}^{mE}}{1-\sqrt{v_f}}G_1 \tag{5.48}$$

$$J_2 = \frac{C_{22}^{mE}}{1-\sqrt{v_f}}F_1 + \frac{\sqrt{v_f}C_{22}^{mE}}{1-\sqrt{v_f}}F_2 - \frac{\sqrt{v_f}C_{23}^{mE}}{1-\sqrt{v_f}}G_2 \tag{5.49}$$

$$J_3 = \frac{C_{23}^{mE}}{1-\sqrt{v_f}}F_1 + \frac{\sqrt{v_f}C_{22}^{mE}}{1-\sqrt{v_f}}F_3 - \frac{\sqrt{v_f}C_{23}^{mE}}{1-\sqrt{v_f}}G_3 \tag{5.50}$$

$$J_4 = e_{32}^{m} + \frac{\sqrt{v_f}C_{22}^{mE}}{1-\sqrt{v_f}}F_4 - \frac{\sqrt{v_f}C_{23}^{mE}}{1-\sqrt{v_f}}G_4 \tag{5.51}$$

Subsequently, considering sub-regions I and II as combined unit in RVE and applying following conditions

$$\sigma_{22}^{c} = \sqrt{v_f}\sigma_{22}^{f} + (1-\sqrt{v_f})\sigma_{22}^{m} \tag{5.52}$$

$$\sigma_{33}^{c} = \sqrt{v_f}\sigma_{33}^{f} + (1-\sqrt{v_f})\sigma_{33}^{m} \tag{5.53}$$

The effective stiffness and piezoelectric coefficients obtained as

$$C_{11}^{c} = \sqrt{v_f}C_{11}^{fE} + \left(1-\sqrt{v_f}\right)C_{11}^{mE} + \sqrt{v_f}\left(C_{12}^{fE} - C_{12}^{mE}\right)F_1 + \sqrt{v_f}\left(C_{13}^{fE} - C_{13}^{mE}\right)G_1 \tag{5.54}$$

$$C_{12}^{c} = C_{12}^{mE} + \sqrt{v_f}\left(C_{12}^{fE} - C_{12}^{mE}\right)F_2 + \sqrt{v_f}\left(C_{13}^{fE} - C_{13}^{mE}\right)G_2 \tag{5.55}$$

$$C_{13}^{c} = C_{13}^{mE} + \sqrt{v_f}\left(C_{12}^{fE} - C_{12}^{mE}\right)F_3 + \sqrt{v_f}\left(C_{13}^{fE} - C_{13}^{mE}\right)G_3 \tag{5.56}$$

$$C_{22}^{c} = \sqrt{v_f}I_2 + (1 - \sqrt{v_f})J_2 \tag{5.57}$$

$$C_{23}^{c} = \sqrt{v_f}I_3 + (1 - \sqrt{v_f})J_3 \tag{5.58}$$

$$C_{33}^{c} = C_{23}^{fE}F_3 + C_{33}^{fE}G_3 \tag{5.59}$$

$$e_{31}^{c} = \sqrt{v_f}e_{31}^{f} + \left(1 - \sqrt{v_f}\right)e_{31}^{m} + \sqrt{v_f}\left(C_{12}^{fE} - C_{12}^{mE}\right)F_4 + \sqrt{v_f}\left(C_{13}^{fE} - C_{13}^{mE}\right)G_4 \tag{5.60}$$

$$e_{32}^{c} = \sqrt{v_f}I_4 + (1 - \sqrt{v_f})J_4 \tag{5.61}$$

$$e_{33}^{c} = e_{33}^{f} + C_{23}^{fE}F_4 + C_{33}^{fE}G_4 \tag{5.62}$$

$$\kappa_{33}^{c} = \sqrt{v_f}\kappa_{33}^{f\epsilon} + \left(1 - \sqrt{v_f}\right)\kappa_{33}^{m\epsilon} + \sqrt{v_f}\left(e_{32}^{f} - e_{32}^{m}\right)F_4 + \sqrt{v_f}\left(e_{33}^{f} - e_{33}^{m}\right)G_4 \tag{5.63}$$

5.3.2 Strain Energy Method

Energy method provides a micromechanics model based on the conservation of strain energy in a piezoelectric fiber reinforced composite subjected to longitudinal loading. Making the same assumptions as for MSM model energy functions for piezoelectric composite, fiber and matrix are given by

$$U^{c} = \int \left\{-\frac{1}{2}\left(\epsilon^{c^T}C^{c^T}\epsilon^{c} + 2E^{c^T}e^{c^T}\epsilon^{c}\right) + \frac{1}{2}E^{c^T}\epsilon^{c^T}E^{c}\right\}dV \tag{5.64}$$

$$U^{f} = \int \left\{-\frac{1}{2}\left(\epsilon^{f^T}C^{f^T}\epsilon^{f} + 2E^{f^T}e^{f^T}\epsilon^{f}\right) + \frac{1}{2}E^{f^T}\epsilon^{f^T}E^{f}\right\}dV \tag{5.65}$$

$$U^{m} = \int \left\{-\frac{1}{2}\left(\epsilon^{m^T}C^{m^T}\epsilon^{m} + 2E^{m^T}e^{m^T}\epsilon^{m}\right) + \frac{1}{2}E^{m^T}\epsilon^{m^T}E^{m}\right\}dV \tag{5.66}$$

Under the given state of stress, the total energy stored in composite is equal to the sum of energies stored in the fiber and the matrix. It can be expressed as

$$U^c = U^f + U^m \tag{5.67}$$

The strain energy term due to mismatch of Poisson's ratio at the fiber/matrix interface is neglected in this approximation approach. Since the neglected terms would be of order square of the difference between the Poisson's ratios of the fiber and the matrix, so the approximation is justified. The strain energy approach allows to model the problem under the consideration of unequal strain generation in fiber and matrix medium due to application of external force in longitudinal as well as in transverse direction.

Stresses and strains in the fibers and the matrix are defined in terms of corresponding composite quantities as given below

$$\sigma_{11}^f = g_1\sigma_{11}^c \tag{5.68}$$

$$\sigma_{11}^m = g_2\sigma_{11}^c \tag{5.69}$$

$$\epsilon_{22}^f = g_3\epsilon_{22}^c \tag{5.70}$$

$$\epsilon_{22}^m = g_4\epsilon_{22}^c \tag{5.71}$$

$$\epsilon_{33}^f = g_5\epsilon_{33}^c \tag{5.72}$$

$$\epsilon_{33}^m = g_6\epsilon_{33}^c \tag{5.73}$$

$$\epsilon_{23}^f = g_7\epsilon_{23}^c \tag{5.74}$$

$$\epsilon_{23}^m = g_8\epsilon_{23}^c \tag{5.75}$$

$$\epsilon_{31}^f = g_9\epsilon_{31}^c \tag{5.76}$$

$$\epsilon_{31}^f = g_9\epsilon_{31}^c \tag{5.77}$$

$$\epsilon_{12}^f = g_{11}\epsilon_{12}^c \tag{5.78}$$

$$\epsilon_{12}^m = g_{12}\epsilon_{12}^c \tag{5.79}$$

$$E_1^f = g_{13}E_1^c \tag{5.80}$$

$$E_1^m = g_{14}E_1^c \tag{5.81}$$

$$E_2^f = g_{15}E_2^c \tag{5.82}$$

$$E_2^m = g_{16}E_2^c \tag{5.83}$$

$$E_3^f = g_{17}E_3^c \tag{5.84}$$

$$E_3^m = g_{18}E_3^c \tag{5.85}$$

Using Eqns. (5.68-5.73), (5.84) and (5.85) following relations are obtained as

$$\epsilon_{11}^f = a_1^f\epsilon_{11}^c + a_2^f\epsilon_{22}^c + a_3^f\epsilon_{33}^c - a_4^f E_3^c \tag{5.86}$$

$$\epsilon_{11}^m = a_1^m\epsilon_{11}^c + a_2^m\epsilon_{22}^c + a_3^m\epsilon_{33}^c - a_4^m E_3^c \tag{5.87}$$

where,

$$a_1^f = \frac{g_1 C_{11}^c}{C_{11}^f} \tag{5.88}$$

$$a_1^m = \frac{g_2 C_{11}^c}{C_{11}^m} \tag{5.891}$$

$$a_2^f = \frac{(g_1 C_{12}^c - g_3 C_{12}^{fE})}{C_{11}^f} \tag{5.90}$$

$$a_2^m = \frac{(g_2 C_{12}^c - g_4 C_{12}^{mE})}{C_{11}^f} \tag{5.91}$$

$$a_3^f = \frac{(g_1 C_{13}^c - g_5 C_{13}^{fE})}{C_{11}^f} \tag{5.92}$$

$$a_3^m = \frac{(g_2 C_{13}^c - g_6 C_{13}^{fE})}{C_{11}^f} \tag{5.93}$$

$$a_4^f = \frac{(g_1 e_{31}^c - g_{17} e_{31}^m)}{C_{11}^f} \tag{5.94}$$

$$a_4^m = \frac{(g_2 e_{31}^c - g_{18} e_{31}^m)}{C_{11}^f} \tag{5.95}$$

Using Eqns. (5.67-5.86) into Eqn. (5.66), equating the coefficients of like terms both side, effective coefficients are obtained as

$$C_{11}^{c} = \frac{C_{11}^{fE} C_{11}^{mE}}{g_1^2 C_{11}^{mE} + g_2^2 C_{11}^{fE}} \tag{5.96}$$

$$C_{12}^{c} = a_1^f g_3 C_{12}^{fE} + a_1^m g_4 C_{12}^{mE} \tag{5.97}$$

$$C_{13}^{c} = a_1^f g_5 C_{13}^{fE} + a_1^m g_6 C_{13}^{mE} \tag{5.98}$$

$$C_{22}^{c} = \frac{\left(g_1 C_{12}^{c} - g_3 C_{12}^{fE}\right)^2}{C_{11}^{f}} + \frac{\left(g_2 C_{12}^{c} - g_4 C_{12}^{fE}\right)^2}{C_{11}^{m}} + g_3^2 C_{22}^{fE} + g_4^2 C_{22}^{mE} + 2a_2^f g_3 C_{12}^{fE} + 2a_2^m g_4 C_{12}^{mE} \tag{5.99}$$

$$C_{23}^{c} = a_3^f g_3 C_{12}^{fE} + a_3^m g_4 C_{12}^{mE} + a_2^f g_5 C_{13}^{fE} + a_2^m g_6 C_{13}^{mE} + g_3 g_5 C_{23}^{fE} + g_4 g_6 C_{23}^{mE} \tag{5.100}$$

$$C_{33}^{c} = \frac{\left(g_1 C_{12}^{c} - g_5 C_{12}^{fE}\right)^2}{C_{11}^{f}} + \frac{\left(g_2 C_{12}^{c} - g_6 C_{12}^{fE}\right)^2}{C_{11}^{m}} + g_5^2 C_{33}^{fE} + g_6^2 C_{33}^{mE} + 2a_3^f g_5 C_{13}^{fE} + 2a_3^m g_6 C_{13}^{mE} \tag{5.101}$$

$$e_{31}^{c} = a_1^f g_{17} e_{31}^{f} + a_1^m g_{18} e_{31}^{m} \tag{5.102}$$

$$e_{32}^{c} = a_2^f g_{17} e_{31}^{f} + a_2^m g_{18} e_{31}^{m} + g_3 g_{17} e_{32}^{f} + g_4 g_{18} e_{32}^{m} + a_4^f g_3 C_{12}^{fE} + a_4^m g_4 C_{12}^{mE} \tag{5.103}$$

$$e_{33}^{c} = a_3^f g_{17} e_{31}^{f} + a_3^m g_{18} e_{31}^{m} + g_5 g_{17} e_{33}^{f} + g_6 g_{18} e_{33}^{m} + a_4^f g_5 C_{13}^{fE} + a_4^m g_6 C_{13}^{mE} \tag{5.104}$$

$$\kappa_{33}^{c} = a_3^f g_{17} e_{31}^{f} + a_3^m g_{18} e_{31}^{m} + g_5 g_{17} e_{33}^{f} + g_6 g_{18} e_{33}^{m} + a_4^f g_5 \kappa_{33}^{f\epsilon} + a_4^m g_6 \kappa_{33}^{m\epsilon} \tag{5.105}$$

It should be noted that constants g_i $(i = 1,2,3 \ldots \ldots 18)$ are experimental parameters and must be obtained through experimental techniques. However, experimental determination of these parameters is out of the scope for the present study. Thus, these parameters are obtained with the theoretical assumptions of modified strength of materials approach as discussed in the previous section. Though fiber is considered for

determination of the effective coefficients through both the above micromechanics models are of the rectangular cross-section but the analysis remains independent of the fiber cross-section. So, it can be concluded that the effective properties derived through these micromechanics models are valid for piezoelectric fiber reinforced composite of any fiber cross-section in general.

5.3.3 Results and Discussion

The equations derived by both the micromechanics methods discussed in the previous sections are used to calculate the numerical values of the effective coefficients as a function of fiber volume fraction. Two different composites having the same matrix materials with different piezoelectric fiber material have been considered for obtaining the numerical values. The results are obtained as plots depicting variation of effective elastic, electric and dielectric properties of PFRC with change in fiber volume fractions. The elastic, electric and dielectric properties of fiber and matrix phases that are used for calculations are shown in Table 5.1.

Table 5.1. Material properties of fiber and matrix phases

Material Prop.	**Epoxy**	**PZT-5H**	**PZT-7A**
C_{11} (GPa)	3.86	151	148
C_{12} (GPa)	2.57	98	76.2
C_{13} (GPa)	2.57	96	74.2
C_{33} (GPa)	3.86	124	131
C_{44} (GPa)	2.57	23	25.4
e_{31} (C/m^2)	0	-5.1	-2.1
e_{33} (C/m^2)	0	27.0	9.5
e_{15} (C/m^2)	0	17.0	9.2
κ_{33} (C/Vm)	0.079×10^{-9}	13.27×10^{-9}	2.07×10^{-9}

The main objective of the present analysis is to study the effect of fiber volume fractions and geometry on effective coefficients of piezoelectric composites. The following non-dimensional parameters are considered for studying the piezoelectric behaviour of the piezoelectric fiber reinforced composites when compared with their monolithic counterpart, i.e., piezoelectric fiber.

$$R_{31} = \frac{e_{31}^{c}}{e_{31}^{f}}, \qquad R_{32} = \frac{e_{32}^{c}}{e_{32}^{f}}, \qquad R_{33} = \frac{e_{33}^{c}}{e_{33}^{f}} \tag{5.106}$$

The effective elastic, piezoelectric and dielectric coefficients of piezoelectric composites calculated by modified strength of materials approach (MSM) and strain energy approach has been compared with those calculated by strength of materials (SM) approach as described in the literature [131,132].

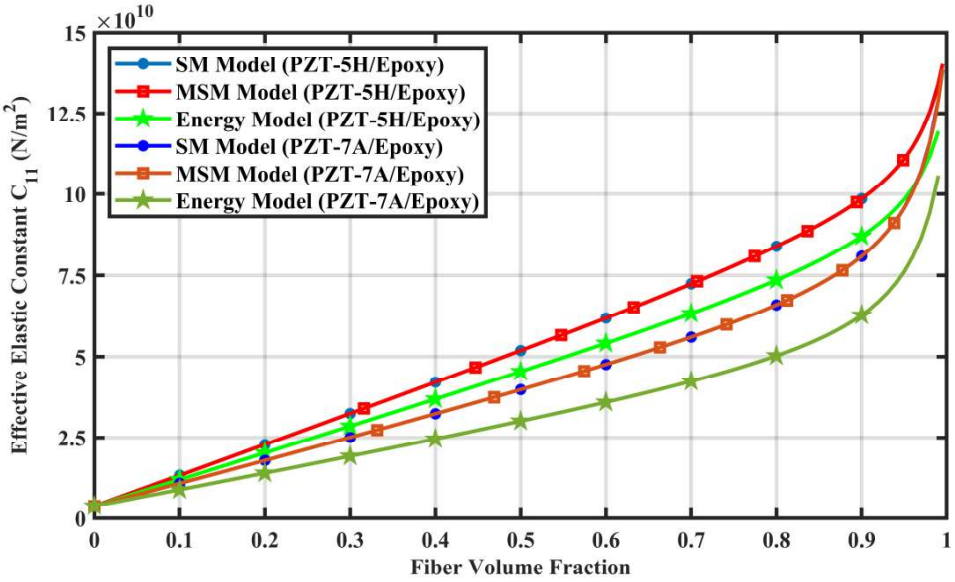

Figure 5.3 The effective elastic coefficient C_{11} as predicted by the model developed in the present study (MSM), SM Model and Energy Model with change in fiber volume fraction.

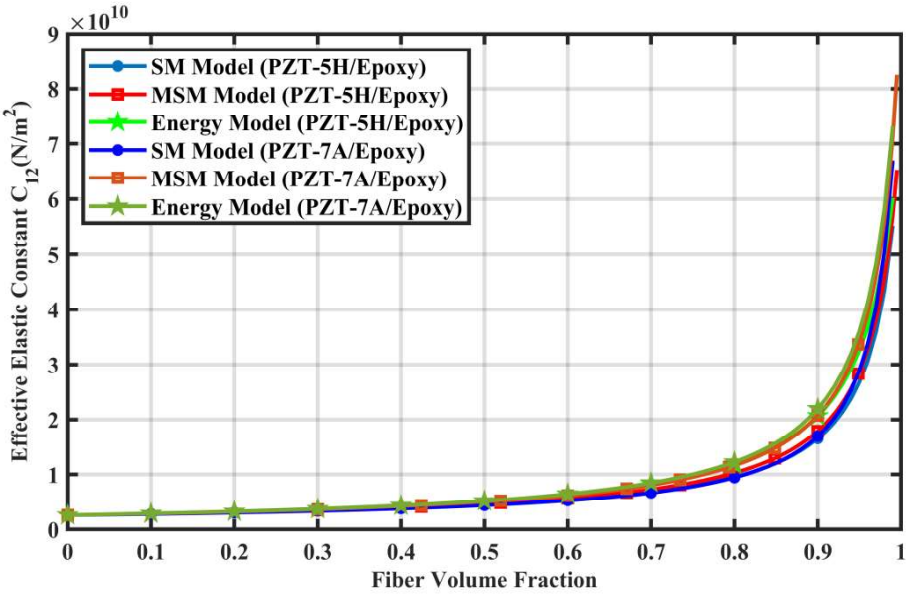

Figure 5.4 The effective elastic coefficient C_{12} as predicted by the model developed in the present study (MSM), SM Model and Energy Model with change in fiber volume fraction.

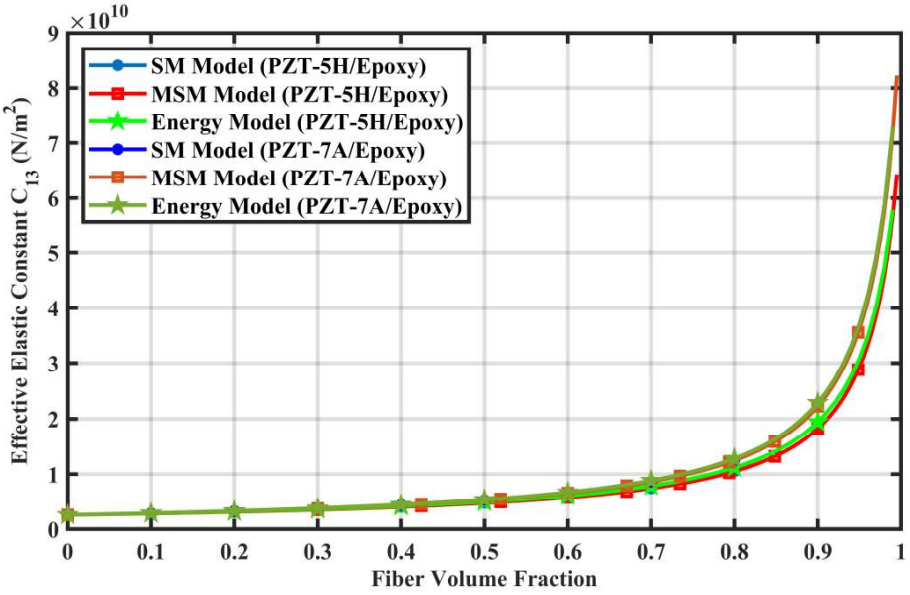

Figure 5.5 The effective elastic coefficient C_{13} as predicted by the model developed in the present study (MSM), SM Model and Energy Model with change in fiber volume fraction.

Figure 5.3 illustrates the variation of the effective elastic coefficient C_{11}^{c} with change in fiber volume fraction. It shows that the values predicted by the strength of materials (SM) approach given in various literature [131-132] and modified strength of materials (MSM) approach developed in the present work are in excellent agreement with each other while the values predicted by the energy method provide an underestimated of values for the whole range of fiber volume fraction. The prediction curves of the effective coefficients show similar pattern for both PZT-5H/Epoxy and PZT-7A/Epoxy composites which leads to the interpretation that material properties of piezoelectric fiber doesn't have any effect on the effective elastic coefficients C_{11}^{c} of the piezoelectric fiber reinforced composites It can also be observed that the underestimation in the values of the effective coefficient C_{11}^{c} as predicted by the energy method is larger for the composite having PZT-7A as fiber than composite having PZT-5H as fiber. The phenomenon of larger degree of underestimation in the predicted values that is observed in composite having PZT-7A fiber material could be attributed to the fact that PZT-7A has a lower C_{11}^{f} value as compared to PZT-5H. In general, the underestimation of the predicted values can be seen as an influence of Poisson's ratio mismatch between the fiber and matrix materials on the overall properties of the composite. It is evident that PZT-5H has higher stiffness than PZT-7A hence the strain energy arises due to the Poisson's ratio mismatch for PZT-5H having lower contribution to the energy terms as compared with PZT-7A. Figures 5.4 and 5.5 show the prediction of the effective elastic coefficients C_{12}^{c} and C_{13}^{c} with change in fiber volume fraction. It is observed that the values predicted by strength of materials (SM) approach, modified strength of materials (MSM) approach and energy approach are in excellent agreement with each other for whole range of fiber volume fractions for both PZT-5H/ Epoxy and PZT-7A/Epoxy composites.

Averaging of strain terms in direction-2 and 3 are employed while deriving the expressions for the effective properties of piezocomposites by SM, MSM and Energy approach but in direction-1 it is assumed to be equal for both fiber and matrix material. While developing modified strength of materials (MSM) model and energy model, since the external loading on the representative volume element (RVE) is applied along direction-1, the effect of fiber packing arrangement and Poisson's ratio mismatch is expected to be the least in directions-2 and 3. The strength of materials (SM) approach described in the literature [131-132] have similar loading conditions, the overlapping of comparison curves occurs for the whole range of fiber volume fraction.

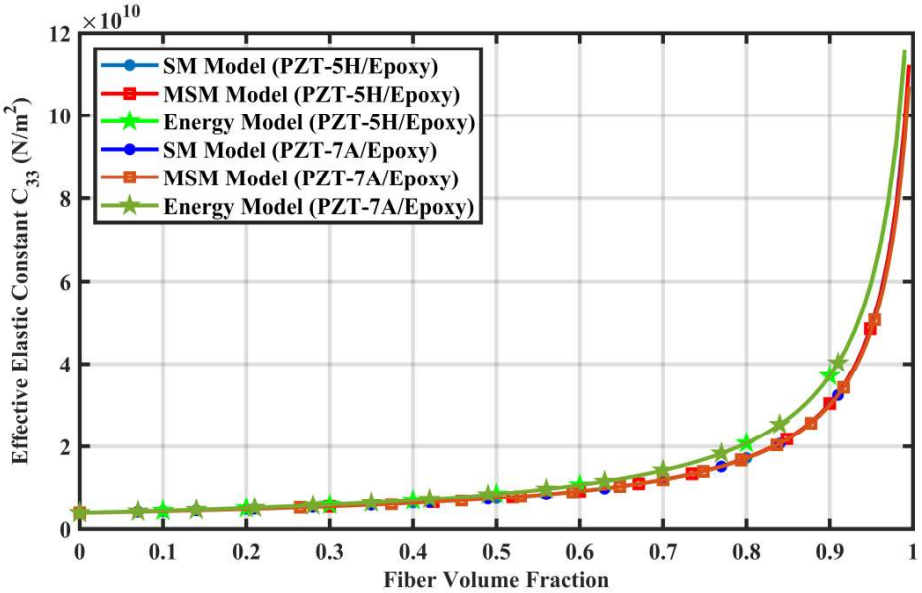

Figure 5.6 The effective elastic coefficient C_{33} as predicted by the model developed in the present study (MSM), SM Model and Energy Model with change in fiber volume fraction.

Figure 5.6 illustrates the variation of the effective elastic coefficient C_{33}^{c} with change in the fiber volume fraction. It shows that the values predicted through energy approach

are in good agreement when compared to those predicted through other two methods, i.e., strength of materials (SM) approach and modified strength of materials (MSM) approach for the useful range of fiber volume fraction (0.1-0.7). For the fiber volume fraction range (>0.6) the values obtained through energy approach shows an overestimation of predicted values when compared to the predicted values obtained through strength of materials (SM) approach and modified strength of materials (MSM) approach. This unusual phenomenon can be attributed to the fact that at higher fiber volume fraction there will be lateral clamping of stiffer fiber rods by the surrounding soft matrix which results in an additional strain energy term contributing to overall strain energy of the composite.

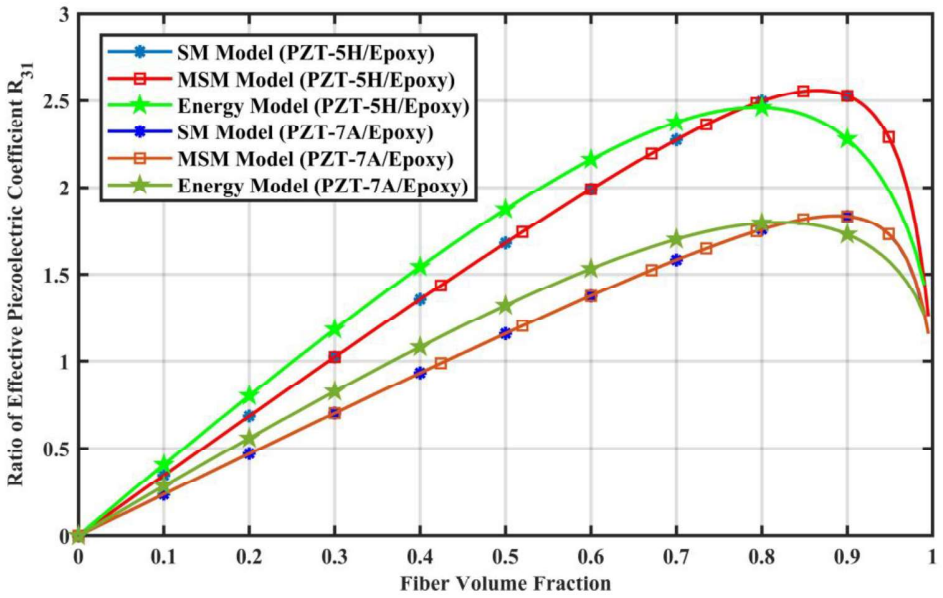

Figure 5.7 Comparison of predicted parameter R_{31} with change in fiber volume fractions.

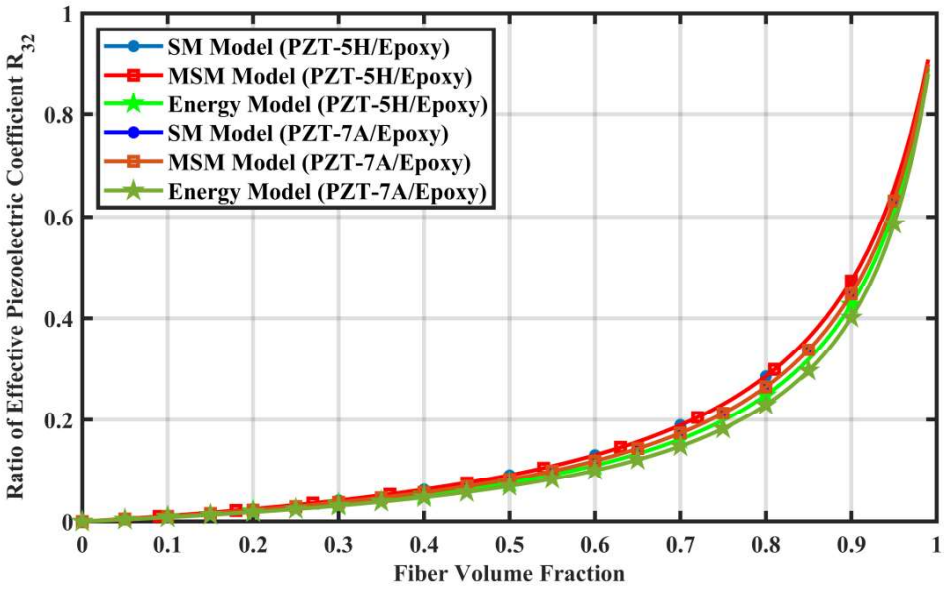

Figure 5.8 Comparison of predicted parameter R_{32} with change in fiber volume fractions.

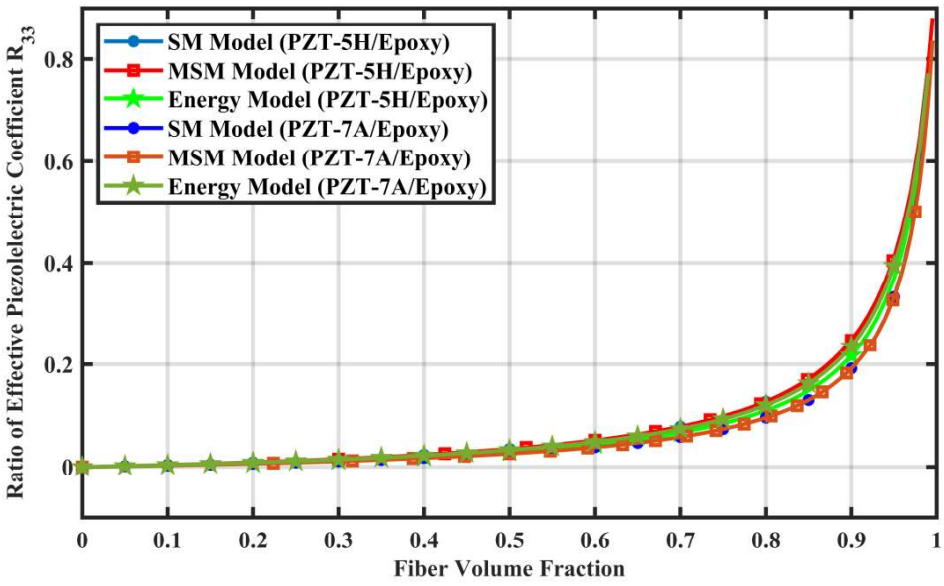

Figure 5.9 Comparison of predicted parameter R_{33} with change in fiber volume fractions.

The variation of the non-dimensional parameters expressed in Eqn. (5.106) as a function of fiber volume fraction is shown in Figures 5.7-5.9. These non-dimensional parameters determine the strength of actuation capabilities of such composites in all the principal directions, i.e., direction-1,2 and 3. The effective piezoelectric coefficient e_{31}^{c} presents a measure of strength of actuation capabilities of a smart material in bending mode when electric field applied is transverse to the fiber direction. Figure 5.7 illustrates that the non-dimensional parameter R_{31} (ratio between overall effective piezoelectric coefficient e_{31}^{c} and piezoelectric coefficient of the fiber e_{31}^{f}) attains values higher than 1 (R_{31}>1) when fiber volume fraction exceeds a critical value (0.3 for PZT-5H/Epoxy and 0.4 for PZT-7A/Epoxy). This shows that there is a significant improvement in the strength of actuation capability in direction-1 of a piezoelectric fiber reinforced composite (PFRC) when electric field is applied in the transverse direction, i.e., direction-3.

The results also suggest that the electrical properties of piezoelectric fiber reinforced composites (PFRC) get enhanced significantly when piezoelectric materials are combined with passive epoxy polymers to obtain such piezocomposite when compared to the monolithic piezoelectric materials. The values predicted by strength of materials (SM) approach and modified strength of materials (MSM) approach are in excellent agreement with each other while the values predicted by energy approach attains comparatively higher values up to 0.8 fiber volume fraction and beyond that inflexion point it attains a lower value when compared to the predicted values by other two approaches.

Figure 5.7 shows that the values predicted through the energy approach reflects significant improvement in actuation capabilities in the useful range of fiber volume

fraction (0.1-0.7) when compared to the predicted values by other two methods. The predicted values for the other two non-dimensional parameters, i.e., R_{32} and R_{33} are shown in figure 5.8 and 5.9. For both these parameters, the values obtained through strength of materials (SM), modified strength of materials (MSM) and energy approach are in an excellent agreement with each other in the useful range of fiber volume fraction (0.1-0.7). The slope of the curves for both these parameters are negative that suggests there is a reduction in the predicted values of the effective piezoelectric constants e_{32}^{c} and e_{33}^{c} for piezoelectric composite when compared to its monolithic counterpart.

These observations suggest that the use of a passive material as matrix (epoxy polymer) in such PFRCs significantly improves their actuation capabilities in direction-1 while it reduces these values of actuation in direction-2 and 3. The reason for the higher value of e_{31}^{c}could be that in such piezocomposites some of the stiffer piezoelectric material (PZT-5H/PZT-7A) gets replaced with soft epoxy material with geometric continuity in direction-1. That's why the actuation capability of the composite in direction-1 due to the electric field in direction-3 attains value higher than its piezo ceramic counterpart (fiber material). However, it should also be noted here that the effective piezoelectric coefficients e_{32}^{c} and e_{33}^{c} are not of much importance because actuation in fiber direction is of the primary concern while designing most of the smart structures.

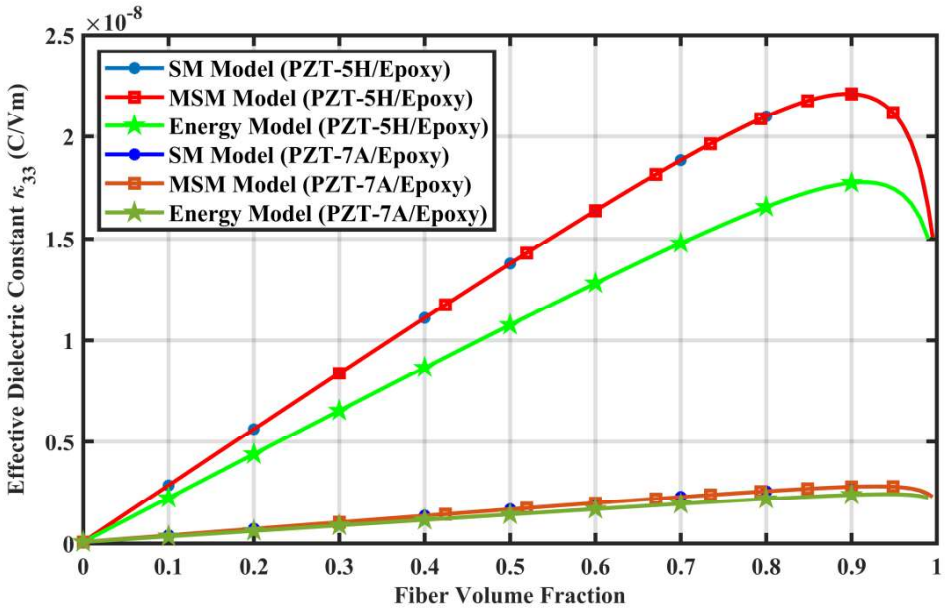

Figure 5.10 The effective dielectric coefficient κ_{33} as predicted by the model developed in the present study (MSM), SM Model and Energy Model with change in fiber volume fraction

The variation of effective dielectric constant κ_{33}^{c} with fiber volume fraction has been illustrated in Figure 5.10. The value predicted through strength of materials (SM) and modified strength of materials (MSM) approach are in excellent agreement with each other for the entire range of fiber volume fraction. But the values predicted by the energy method attain significantly lower values than those obtained by strength of materials (SM)and modified strength of materials (MSM) approaches. It is also observed from the figure that the gap in the predicted values by energy method when compared to other two methods is small for PZT-7A/epoxy piezocomposite as compared to PZT-5H/epoxy piezocomposite. The reason for this could be that the ratio for the dielectric constant in direction-3 for the fiber and matrix materials, i.e., $\kappa_{33}^{f}/\kappa_{33}^{m}$, is much higher for PZT-

5H/epoxy piezocomposite (=167.975) as compared to PZT-7A/epoxy piezocomposite (=26.203).

5.4 Numerical Model

5.4.1 Finite Element Method (FEM)

A unit cell-based finite element model has been adopted by various Berger *et. al.* and Aboudi [121,122,133] to study the effect of fiber geometry on the overall material properties. A unit cell-based micromechanics model more often contains a representative volume element (RVE) of the bulk material which contains both fiber and matrix phases. In general, this approach involves the following five steps.

i. An appropriate unit cell containing sufficient information of both fiber and matrix phases is identified for a specified fiber volume fraction.
ii. The unit cell is subjected to mechanical and electrical loading constraints under the designated boundary conditions.
iii. The resultant stress and electric field components are measured that developed due to applied boundary conditions.
iv. A homogenized coupled response is captured by invoking an appropriate averaging technique.
v. All the effective coefficients are calculated by using representation of the coupled response of piezoelectric materials shown by Eqn. 5.1 (a)-(c).

5.4.2 Periodic Boundary Conditions

The bulk composite materials can be represented as a periodical array of RVEs. By coupling opposite nodes on opposite boundary surfaces of RVE, periodic boundary conditions are formulated [141]. It is assumed that each RVE in the composite has the

same deformation mode and there is no overlap or separation between adjacent RVEs. Mathematically, these conditions can be described as follows

$$u_i = \bar{\epsilon}_{ij} x_j + v_i \tag{5.107}$$

In Eqn. (5.107) $\bar{\epsilon}_{ij}$ are the average strains, v_i are the periodic local fluctuations on the boundary surfaces as a result of the applied global loads. The indices $(i, j = 1,2,3)$ represents a global three-dimensional coordinate system. A RVE containing square array of periodic cylindrical fiber embedded in soft matrix is shown in Figure 5.1 (b). Using Eqn. (5.107), the periodic boundary conditions can be obtained in more explicit form. The displacement on a pair of opposite boundary surfaces with their normal, along x_j-axis is given by

$$u_i^{K^+} = \bar{\epsilon}_{ij} x_j^{K^+} + v_i^{K^+} \tag{5.108}$$

$$u_i^{K^-} = \bar{\epsilon}_{ij} x_j^{K^-} + v_i^{K^-} \tag{5.109}$$

where $K^{+/-}$ denotes direction along positive/negative x_j-axis on the corresponding opposite surfaces, i.e. A^+/A^-, B^+/B^- and C^+/C^-. As boundary conditions are periodic in nature, the local fluctuations $v_i^{K^+}$ and $v_i^{K^-}$ remains identical in the global coordinate system. The applied macroscopic strain condition can be written as

$$u_i^{K^+} - u_i^{K^-} = \bar{\epsilon}_{ij}(x_j^{K^+} - x_j^{K^-}) \tag{5.110}$$

Similarly, applied macroscopic electric field due to periodic boundary condition can be written as

$$\phi^{K^+} - \phi^{K^+} = \bar{E}_i(x_j^{K^+} - x_j^{K^-}) \tag{5.111}$$

Now, the volume average of mechanical and electrical properties of the RVE will give the prediction about the average properties of the bulk composite. The average stresses and strains in RVE are defined by

$$\bar{\epsilon}_{ij} = \frac{1}{V}\int_V \epsilon_{ij} dV \tag{5.112}$$

$$\bar{\sigma}_{ij} = \frac{1}{V}\int_V \sigma_{ij} dV \tag{5.113}$$

where V is the volume of the periodic RVE. And, average electric fields and electric displacements are defined as

$$\bar{E}_i = \frac{1}{V}\int_V E_i dV \tag{5.114}$$

$$\bar{D}_i = \frac{1}{V}\int_V D_i dV \tag{5.115}$$

Thus, all the effective coefficients of piezo composite can be derived as the ratio of corresponding average stresses and strains generated due to applied load conditions along with above mentioned periodic boundary conditions at surface nodes of the representative volume element (RVE).

5.4.3 Calculation of Effective Coefficients through FEM

The numerical calculations were performed with FE software ANSYS on a workstation platform. The matrix and fiber phases were meshed with 20 node 186 and 20 node 226 tetrahedron elements with full integration. To get homogenized material properties, periodic boundary conditions were generated by coupling the nodes of the opposite boundary surfaces of the RVE. Berger *et. al.* [121] used a FORTRAN programme to generate these boundary conditions. Similar boundary conditions are developed in parametric design language of the software by using the described approach. A constraint equation needs to be imposed for each pair of displacement or field components of two corresponding nodes of opposite surfaces with similar in-plane coordinates. In order to get these constraints, meshes with triangular elements are generated on areas of three adjacent orthogonal surfaces of the RVE, then these meshes

are copied to the exactly opposite surfaces. This will help in generating two similar in-plane coordinates on opposite surfaces of the RVE. After that, the fiber and the matrix volume are meshed separately followed by deletion of area meshes generated on all the six surfaces of the RVE. Poizat *et. al.* in [60] have reported that mesh sizes of as fine as about 1000 elements are sufficient to study the electro-elastic problems related to the 0-3 piezoelectric composite. A convergence study was carried out to find the ideal mesh size and it was found that the mesh with 5704 elements was fine enough to represent geometry of fiber and matrix effectively and reduce aberrations in the calculation of the overall properties of the piezo composite (see Figure 5.11).

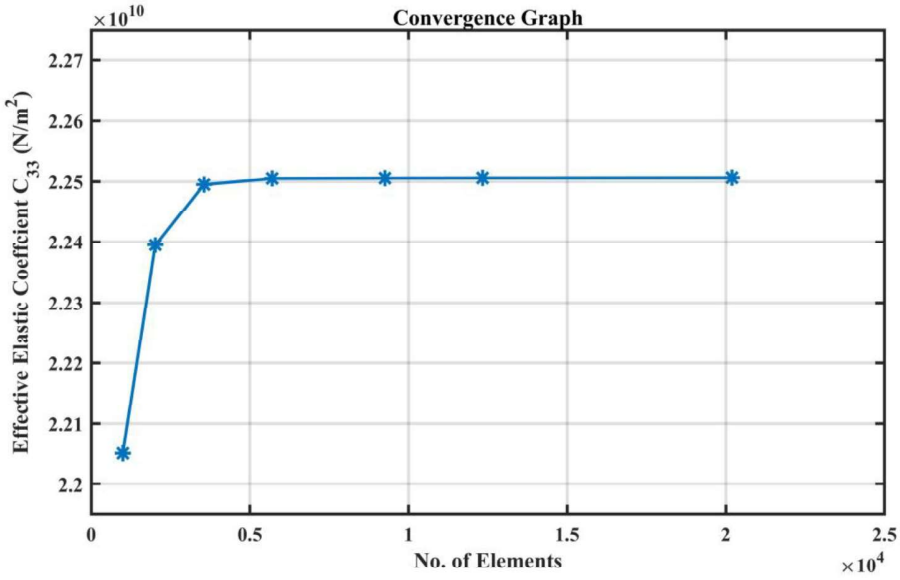

Figure 5.11 The convergence graph for determining ideal mesh size for the FE analysis.

The boundary conditions are applied as stated in the previous section and the results are calculated with the help of ANSYS integrated solver which lists the stress and strains for each node and element. The macro parameters are obtained from the weighted average value of the stresses, strains and electric displacements as shown in Eqns. (5.112-

5.115). The material properties of the constituents taken for both the calculations, i.e., analytical model and numerical model are listed in Table 5.2.

Table 5.2: Material properties of the fiber and matrix phases for FEM calculations

Material Properties	**Epoxy (Matrix)**	**PZT-5 (Fiber)**
C_{11}	3.86 GPa	121 GPa
C_{12}	2.57 GPa	75.4 GPa
C_{13}	2.57 GPa	75.2 GPa
C_{33}	3.86 GPa	111 GPa
C_{44}	0.64 GPa	21.1 GPa
C_{66}	0.64 GPa	22.8 GPa
e_{31}	--	-5.4 (C/m^2)
e_{33}	--	15.8 (C/m^2)
e_{15}	--	12.3 (C/m^2)
κ_{11}	0.079×10^{-9} (C/Vm)	8.11×10^{-9} (C/Vm)
κ_{33}	0.079×10^{-9} (C/Vm)	7.35×10^{-9} (C/Vm)

Every load case is calculated for six sets of fiber volume fraction ranging from 0.1 to 0.6 with sub steps of 0.1. Figure 5.12 shows RVE of these six different sets of fiber volume fraction where the edge of the RVE is of unit length. For numerical calculations based on the unit cell method, the matrix representation of Eqns. 5.2 (a)-(b) can be modified into

$$\begin{Bmatrix} \langle\sigma_{11}\rangle \\ \langle\sigma_{22}\rangle \\ \langle\sigma_{33}\rangle \\ \langle\sigma_{23}\rangle \\ \langle\sigma_{31}\rangle \\ \langle\sigma_{12}\rangle \\ \langle D_1\rangle \\ \langle D_2\rangle \\ \langle D_3\rangle \end{Bmatrix}$$

$$= \begin{bmatrix} C_{11}^{eff} & C_{12}^{eff} & C_{13}^{eff} & 0 & 0 & 0 & 0 & 0 & -e_{31}^{eff} \\ C_{12}^{eff} & C_{11}^{eff} & C_{13}^{eff} & 0 & 0 & 0 & 0 & 0 & -e_{31}^{eff} \\ C_{13}^{eff} & C_{13}^{eff} & C_{33}^{eff} & 0 & 0 & 0 & 0 & 0 & -e_{33}^{eff} \\ 0 & 0 & 0 & C_{44}^{eff} & 0 & 0 & 0 & -e_{15}^{eff} & 0 \\ 0 & 0 & 0 & 0 & C_{44}^{eff} & 0 & -e_{15}^{eff} & 0 & 0 \\ 0 & 0 & 0 & 0 & 0 & C_{66}^{eff} & 0 & 0 & 0 \\ 0 & 0 & 0 & 0 & e_{15}^{eff} & 0 & \kappa_{11}^{eff} & 0 & 0 \\ 0 & 0 & 0 & e_{15}^{eff} & 0 & 0 & 0 & \kappa_{11}^{eff} & 0 \\ e_{31}^{eff} & e_{31}^{eff} & e_{33}^{eff} & 0 & 0 & 0 & 0 & 0 & \kappa_{33}^{eff} \end{bmatrix} \begin{Bmatrix} \langle\epsilon_{11}\rangle \\ \langle\epsilon_{22}\rangle \\ \langle\epsilon_{33}\rangle \\ \langle\epsilon_{23}\rangle \\ \langle\epsilon_{31}\rangle \\ \langle\epsilon_{12}\rangle \\ \langle E_1\rangle \\ \langle E_2\rangle \\ \langle E_3\rangle \end{Bmatrix}$$

(5.116)

With the help of above mathematical relation, the overall behaviour of the piezoelectric composite can be evaluated in terms of the effective elastic constants C_{ijkl}^{eff}, the effective piezoelectric constants e_{ikl}^{eff} and the effective dielectric constants κ_{ik}^{eff}. $\langle \dots \rangle$ denotes the spatial average value for directional stresses and strains.

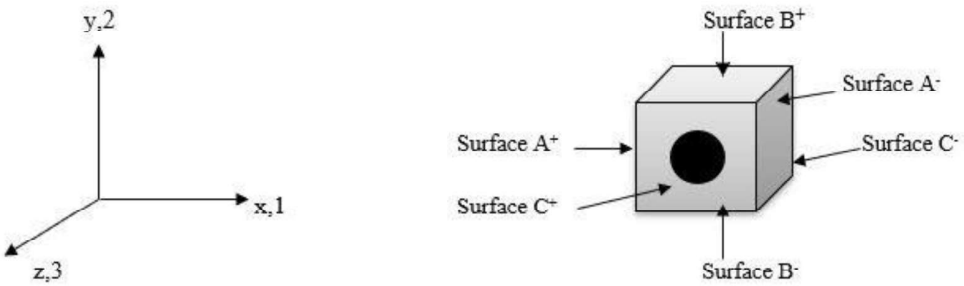

Figure 5.1(b) A representative volume element (RVE) showing boundary surfaces

Table 5.3 List of boundary conditions applied on RVE and formula for calculation of effective coefficients

Eff. Coeff.	**A⁻** u_i/ϕ	**A⁺** u_i/ϕ	**B⁻** u_i/ϕ	**B⁺** u_i/ϕ	**C⁻** u_i/ϕ	**C⁺** u_i/ϕ	**Formula**
C_{11}^{eff}	$0/-$	$\tilde{u}_1/-$	$0/-$	$0/-$	$0/0$	$0/0$	$\langle\sigma_{11}\rangle/\langle\epsilon_{11}\rangle$
C_{12}^{eff}	$0/-$	$\tilde{u}_1/-$	$0/-$	$0/-$	$0/0$	$0/0$	$\langle\sigma_{22}\rangle/\langle\epsilon_{11}\rangle$
C_{13}^{eff}	$0/-$	$0/-$	$0/-$	$0/-$	$0/0$	$\tilde{u}_3/-$	$\langle\sigma_{11}\rangle/\langle\epsilon_{33}\rangle$
C_{33}^{eff}	$0/-$	$0/-$	$0/-$	$0/-$	$0/0$	$\tilde{u}_3/-$	$\langle\sigma_{33}\rangle/\langle\epsilon_{33}\rangle$
C_{44}^{eff}	$(\tilde{u}_3)/0$	$(\tilde{u}_3)/0$	$0/-$	$0/-$	$(\tilde{u}_1)/-$	$(\tilde{u}_1)/-$	$\langle\sigma_{13}\rangle/\langle\epsilon_{31}\rangle$
C_{66}^{eff}	$(\tilde{u}_2)/0$	$(\tilde{u}_2)/0$	$(\tilde{u}_1)/0$	$(\tilde{u}_1)/0$	$0/0$	$0/0$	$\langle\sigma_{12}\rangle/\langle\epsilon_{12}\rangle$
e_{31}^{eff}	$0/-$	$0/-$	$0/-$	$0/-$	$0/0$	$0/\tilde{\phi}$	$-\langle\sigma_{11}\rangle/\langle E_3\rangle$
e_{33}^{eff}	$0/-$	$0/-$	$0/-$	$0/-$	$0/0$	$0/\tilde{\phi}$	$-\langle\sigma_{33}\rangle/\langle E_3\rangle$
e_{15}^{eff}	$(\tilde{u}_3)/0$	$(\tilde{u}_3)/0$	$0/-$	$0/-$	$(\tilde{u}_1)/-$	$(\tilde{u}_1)/-$	$\langle D_1\rangle/\langle\epsilon_{31}\rangle$
κ_{11}^{eff}	$0/0$	$0/\tilde{\phi}$	$0/-$	$0/-$	$0/-$	$0/-$	$\langle D_1\rangle/\langle E_1\rangle$
κ_{33}^{eff}	$0/-$	$0/-$	$0/-$	$0/-$	$0/0$	$0/\tilde{\phi}$	$\langle D_3\rangle/\langle E_3\rangle$

Table 5.3 represents a summary of boundary conditions given to adjacent surfaces of the representative volume element (RVE) (shown in Figure 5.1(b)) and the last column of the table indicates the ratio of average elemental values of respective directional properties that determines the effective coefficients of the piezoelectric composites.

The different configurations of the applied boundary condition can be explained as follows:

- "0" denotes a prescribed zero displacement or electric potential.
- "$\tilde{u}_i$" denotes a non-zero prescribed displacement for the component u_i.
- "$\tilde{\phi}$" denotes a non-zero prescribed electric potential $\tilde{\phi}$.
- "$(\tilde{u}_i)$" denotes a constraint of coupling with the opposite surface for displacement component u_i.

For calculating the effective coefficients C_{13}^f and C_{33}^f the boundary conditions as prescribed in Table 5.3 will be applied to the RVE in such a way that only the strain in x_3-direction, ϵ_{33}, is a non-zero component leaving all other mechanical strains and electric field zero. This condition is achieved by constraining the normal displacement of all other surfaces of RVE to be equal to zero except those for the surface C^+. The periodic boundary conditions are fulfilled for A^-/A^+ and B^-/B^+ surfaces according to the Eqn. (5.110) because of prescribed normal displacement to these surfaces being zero. Since, the normal displacement associated with the surface C^- in x_3-direction has also got its value zero, the periodic boundary conditions in the given direction according to the Eqn. (5.110) reduces to

$$u_3^{C^+} = \langle \epsilon_{33} \rangle (x_3^{C^+} - x_3^{C^-}) \tag{5.117}$$

Now, to produce a strain in x_3-direction any arbitrary constant prescribed displacement is applied to the surface C^+. For simplification a unit displacement is used while calculating the effective coefficients. To make the electric field $\langle E_3 \rangle$ zero, the voltage degree of freedom ϕ is also constrained to zero for the surface C^-/ C^+. The total average values $\langle \epsilon_{33} \rangle$, $\langle \sigma_{11} \rangle$ and $\langle \sigma_{33} \rangle$ are calculated by replacing the integral shown in Eqn. (5.112) and (5.113) with a sum over average elemental values multiplied by the volume of the RVE. Using these total average values, the effective coefficients C_{13}^f and C_{33}^f can be calculated according to the formula shown in Table 5.3. Since all the strains

and electric fields are zero, except $\langle \epsilon_{33} \rangle$, the first row of the matrix shown in Eqn. (5.116) becomes $\langle \sigma_{11} \rangle = C_{13}^{f} \langle \epsilon_{33} \rangle$. Then, C_{13}^{f} is calculated by taking the ratio of $\langle \sigma_{11} \rangle / \langle \epsilon_{33} \rangle$. Similarly, the value of effective coefficient can be predicted by taking the ratio of $\langle \sigma_{33} \rangle / \langle \epsilon_{33} \rangle$ from the third row of the matrix. Using the formula given in Table 5.3, all other coefficients that use average normal strain can be evaluated conveniently.

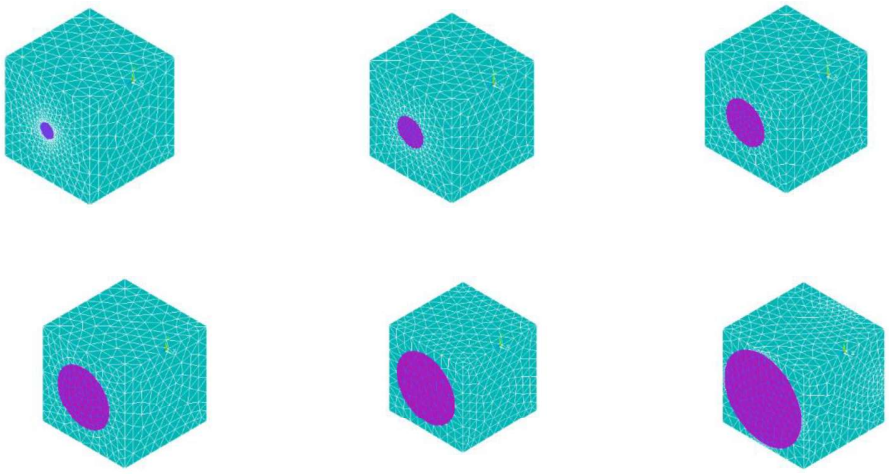

Figure 5.12(a) RVE of finite element analysis (FEA): Fiber volume fractions (0.1-0.6 with step size of 0.1) taken to evaluate effective properties.

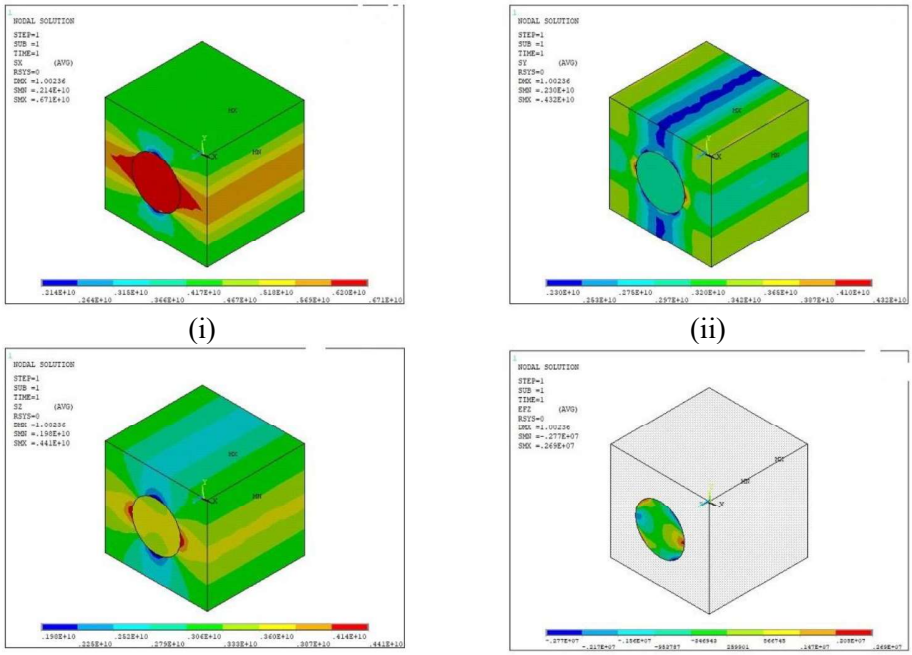

(i) (ii)

(iii) (iv)

Figure 5.12(b) The distribution of stress/electric field in the RVE when the mechanical load (in z-direction) and boundary conditions are applied; **(i)** stress in direction-1 (x-axis); **(ii)** stress in direction-2 (y-axis); **(iii)** stress in direction-3 (z-axis); **(iv)** electric field distribution in direction-3 (z-axis).

For the value of fiber volume fraction of 0.3, the distribution of stresses and strains are shown in Figure 5.12 (b)-(c) and the calculated electric field distribution is shown in Figure 5.12 (d). The calculation for the effective coefficients such as C_{44}^{eff}, C_{66}^{eff} and e_{15}^{eff} depends on the averaged shear strains. For this purpose, the coupling constraint on the two pairs of the opposite surfaces must be defined appropriately. The effective coefficient C_{66}^{eff} which depends on pure in-plane (x_1-x_2 plane) shear stress, the constraint

equation for a pair of nodes on the opposite surfaces A^-/ A^+ can be written according to Eqn. (5.113) as

$$u_2^{A^+} = u_2^{A^-} + \langle \epsilon_{12} \rangle (x_1^{A^+} - x_1^{A^-}). \tag{5.118}$$

The fluctuating part, i.e., $\langle \epsilon_{12} \rangle (x_1^{A^+} - x_1^{A^-})$ is assigned a unitary value. An analogous constraint equation is also defined for the pair of surfaces C^-/ C^+. An additional constraint is applied to avoid any rigid body movement by fixing the edge at the intersection of surfaces $B^-$and C^- in the x_1 and x_2 directions. Similarly, the effective coefficients C_{44}^{eff} and e_{15}^{eff} are calculated by replicating the constraint condition based on the pure out-of-plane shear stress. Based on the boundary conditions listed in Table 5.3, it is observed that only a set of six calculations are necessary to obtain all 11 coefficients. These six groups have been summarized in Table 5.4.

Table 5.4 Classifications of coefficients in groups according to the boundary conditions used for FEM analysis

Group	**1**	**2**	**3**	**4**	**5**	**6**
Eff. Coeff.	C_{11}^{eff},C_{12}^{eff}	C_{13}^{eff},C_{33}^{eff}	C_{44}^{eff},e_{15}^{eff}	C_{66}^{eff}	C_{31}^{eff},C_{33}^{eff},κ_{33}^{eff}	κ_{11}^{eff}

5.4.4 Results and Discussion

The effective electro-elastic coefficients have been calculated using a micromechanics approach viz. improved mechanics of solid and a finite element approach using FE software ANSYS 18.0. The effective coefficients of 1-3 piezoelectric composite have been analysed for six different sets of discrete fiber volume fraction ranging from 0.1 to 0.6. A comparison graph has been obtained by interpolating the results obtained at those six discrete volume fraction points. In literature a strength on materials based (SM)

approach has been presented by [131] to evaluate the effective electro-elastic coefficient of the effective electro-elastic coefficient of piezoelectric fiber reinforced composite (PFRC). Kumar *et. al.* in [132] uses a similar approach to study the thermal responses of such piezo composite by using the similar approach based of strength of materials. The analytical model developed in the current study uses an improved version of that approach described in [142]. The analytical model stated in the [142] provides solutions to the problems related to elastic behaviour only, the model developed in the current study uses that approach to derive solutions for problems related to the electro-elastic behaviour.

The effective electroelastic coefficients have been derived and the numerical results have been calculated for six different sets of fiber volume fractions ranging from 0.1-0.6 and results have been compared to those obtained from finite element approach. Finite element method has been used effectively by [121,122,135] to model similar problems but the FEM approach adopted in the present study uses a different meshing technique to mesh the unit cell (RVE). The number of elements taken for numerical calculations are also very high (in range of over 5000) so as to capture the local field fluctuation effectively as compared to earlier approaches. The variation of the effective material constants has been plotted as a function of fiber volume fraction with results derived from analytical and numerical solutions. The plots have been obtained for conventional strength of materials (SM) approach, analytical model developed based on micromechanics approach, viz. modified strength of materials (MSM) approach and numerical solution obtained through finite element method (FEM). These results have been illustrated by interpolating the outcome of the analysis carried out on six different sets of fiber volume fraction (0.1-0.6).

From Figure 5.13-5.15, it is observed that for effective elastic coefficients C_{11}^c, C_{12}^c, C_{13}^c, the values obtained through the present micromechanics approach are higher

than the values estimated through strength of materials (SM) approach but lower than those estimated through finite element method (FEM). In all these predicted results the values estimated through the strength of material (SM) and finite element approach (FEM) forms lower and upper bounds for the values estimated through micromechanics model developed in present work, i.e., modified strength of material (MSM) approach. The divergence in results toward the upper range of fiber volume fractions is more prominent for the effective elastic coefficients C_{11}^{c} as compared with the other two. It is observed from Figure 5.13 that the values calculated by the present micromechanics model based on modified strength of materials approach attains almost the same values as calculated by numerical method (FEM). It can also be observed from the plots that the values estimated through all three methods have concurrence at lower fiber volume fraction (0.1-0.3) but the values diverge at higher range of the fiber volume fraction (0.3-0.6).

The effective elastic coefficient C_{33}^{c} shows a linear response for the entire range of fiber volume fraction as predicted by all three methods. Figure 5.16 illustrates that the strength of materials (SM) approach overpredicts the values while the values predicted by micromechanics model based on modified strength of materials approach and finite element method, though having slightly lower values that SM approach, are in reasonable agreement with each other. Contrary to the divergence towards upper range of fiber volume fraction as observed for other effective elastic coefficients, the divergence observed for the effective elastic coefficient C_{33}^{c} is for the entire working range of fiber volume fraction (0.1-0.6).

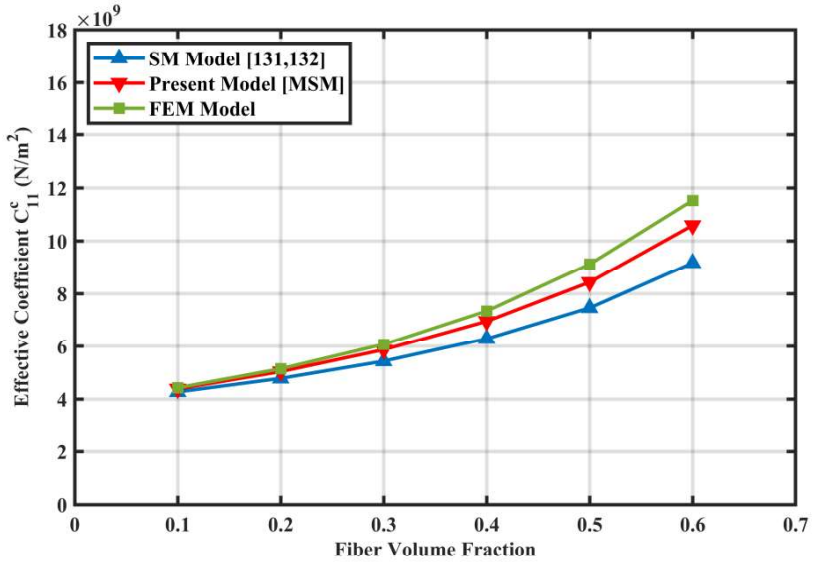

Figure 5.13 The predicted effective elastic coefficient C_{11}^{c} with change in fiber volume fraction by strength of materials model, present micromechanics model and FEM model.

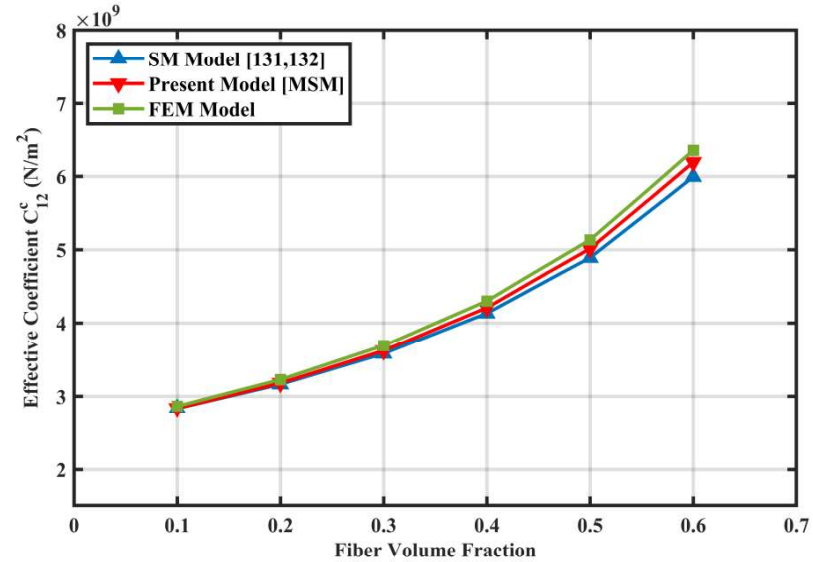

Figure 5.14 The predicted effective elastic coefficient C_{12}^{c} with change in fiber volume fraction by strength of materials model, present micromechanics model and FEM model.

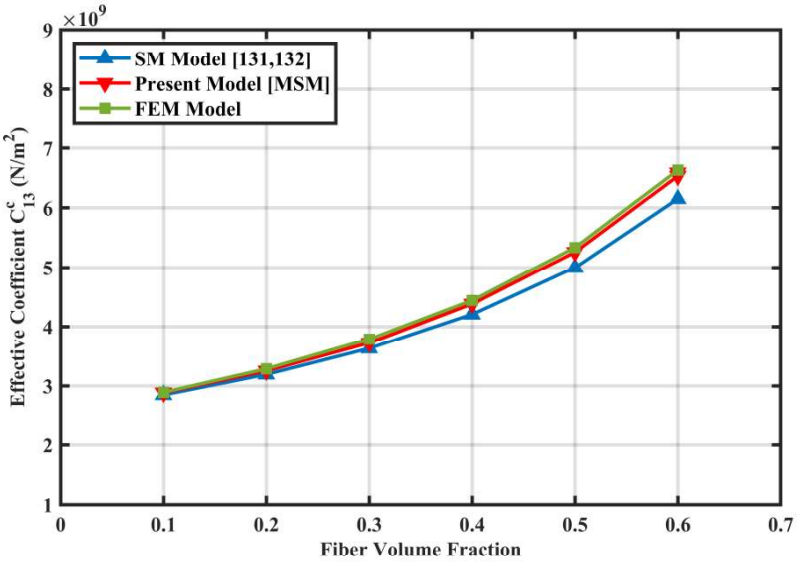

Figure 5.15 The predicted effective elastic coefficient C_{13}^{c} with change in fiber volume fraction by strength of materials model, present micromechanics model and FEM model.

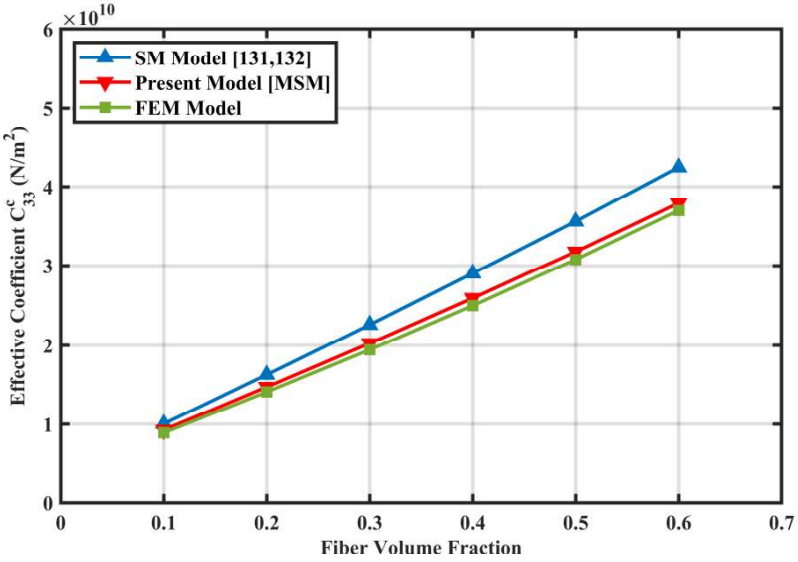

Figure. 5.16 The predicted effective elastic coefficient C_{33}^{c} with change in fiber volume fraction by strength of materials model, present micromechanics model and FEM model.

Figure 5.17-5.18 shows the comparison of results predicted by strength of materials (SM) approach, the present micromechanics approach and the finite element-based approach for the effective piezoelectric coefficients e_{31}^{c} and e_{33}^{c} . It is observed from the Figure 5.17 that predicted value of the is in agreement with each other for all the three models for the entire range of fiber volume fraction through a negligible divergence in predicted value is observed at the higher end of the fiber volume fraction. Figure 5.18 shows that for the effective piezoelectric coefficient, e_{33}^{c} , the predicted values through micromechanics approach and finite-element based approach are in agreement with each other while the values predicted by strength of materials (SM) approach are underestimated for the entire range of the fiber volume fraction.

For both the effective piezoelectric coefficients the values predicted by conventional strength of materials (SM) approach and finite-element based approach forms lower and upper bounds, respectively. FEA involves analysis over RVE of discrete volume fractions (0.1-0.6) for which similar steps are repeated over multiple times which makes it very time consuming and uneconomical. Moreover, at the very higher ends of fiber volume fractions it would be difficult to mesh the RVE at interphases so the final estimated value would not be so precise. MSM approach provides the exact solutions in form of expressions for the effective electroelastic properties which are quite effective in predicting values for the whole range of the fiber volume fractions.

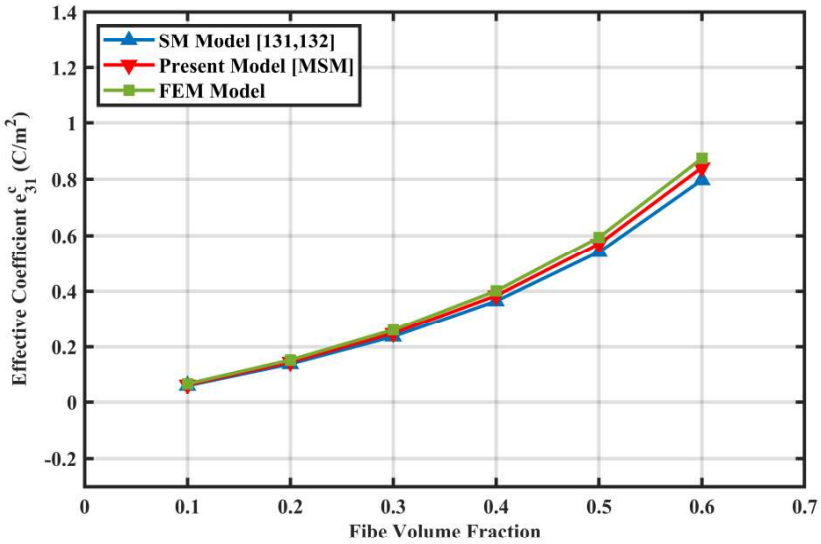

Figure 5.17 The predicted effective piezoelectric coefficient e_{31}^c with change in fiber volume fraction by strength of materials model, present micromechanics model and FEM model.

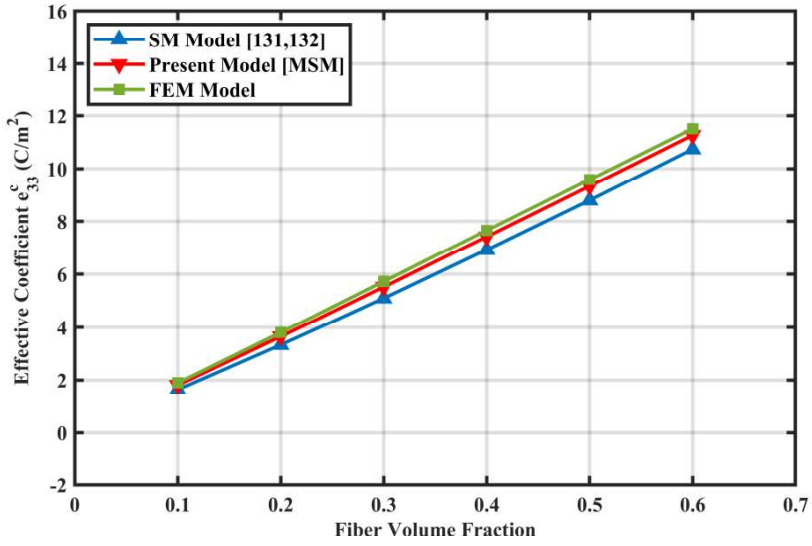

Figure 5.18 The predicted effective piezoelectric coefficient e_{33}^c with change in fiber volume fraction by strength of materials model, present micromechanics model and FEM model.

Figure 5.19 shows that the values of effective dielectric constant κ_{33}^{c} predicted through micromechanics model developed in the present work is in good agreement with those predicted through FEM model. Though the predicted values show a linear nature throughout the working range of fiber volume fraction (0.1-0.6) for all three models, the values predicted by conventional strength of materials (SM) remain underestimated throughout the range of fiber volume fraction.

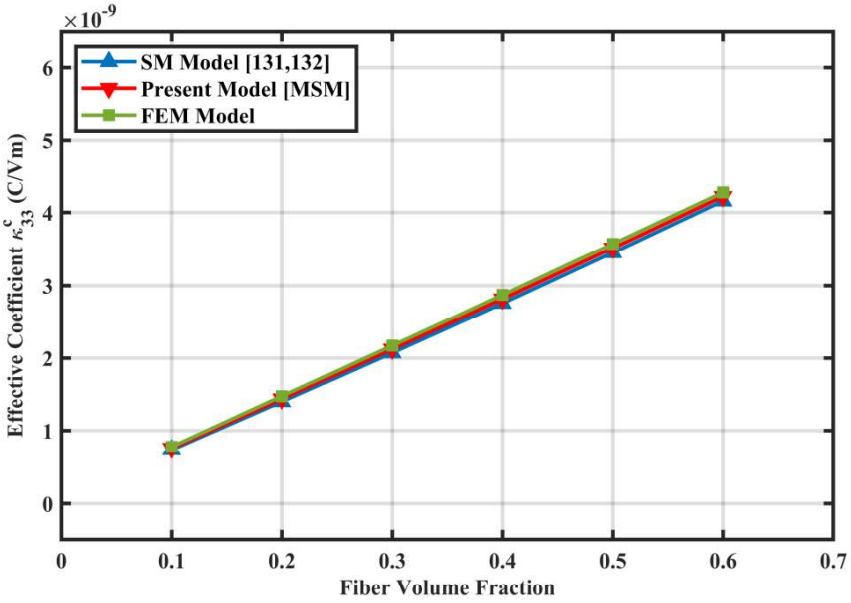

Figure 5.19 The predicted effective dielectric constant κ_{33}^{c} with change in fiber volume fraction by strength of materials model, present micromechanics model and FEM model

Qualitatively, the behaviour of all coefficients calculated show similar nature throughout the range of fiber volume fraction but the coefficients that are influenced by in-plane behaviour shows more convergence in the estimated values. For all the effective coefficients the values predicted through improved mechanics of solid approach shows greater concurrence with the values predicted through the finite element approach (FEM).

However, the values predicted through conventional strength of materials (SM) approach is underestimated or overestimated for most of the effective coefficients. This may be attributed to the fact that the assumed transverse isotropy while modelling the problem with strength of materials (SM) approach is not fulfilled exactly for PFRCs containing of fibers in square packing arrangement, because there is an obvious difference in fiber distance from the centre of RVE in the perpendicular and diagonal directions. While many of the analytical models based their study on this assumption, the present micromechanics model based on modified strength of materials reduces this aberration by the modification in area of the fiber cross-section to that of the equivalent area of a square. Since, in the finite element-based model, the real fiber arrangements are reflected in geometry the results obtained through FEM may be taken as reference to compare the accuracy of the results.

5.5 Summary

In this chapter, two distinct studies are carried out to understand the effects of transverse loading conditions and fiber packing arrangement on the overall properties of piezoelectric fiber reinforced composite. In the first part of the study, analytical models based on modified strength of materials (MSM) approach and strain energy approach have been developed to study the effective properties of piezoelectric fiber reinforced composites. Both these models are capable of predicting effective elastic, piezoelectric and dielectric properties of a piezocomposite subjected to electro-elastic loadings. Even though evaluation of effective electro-elastic coefficients of a piezocomposite have been reported earlier, the model developed in the current study is capable of mapping the effects of fiber packing arrangements and Poisson's ratio mismatch at fiber/matrix interphase on the effective coefficients of piezocomposites. The results obtained through modified strength of materials (MSM) and energy approach have been compared with

strength of materials (SM) approach discussed widely in the literature. The outcome of the first part of the study can be summed up in the following points:

i. The values of the effective elastic, piezoelectric and dielectric coefficients predicted by strength of materials (SM) approach and modified strength of materials (MSM) approach are in good agreement with each other for the whole range of fiber volume fraction for all the effective coefficients but the values predicted by energy method provides an underestimation for all the effective coefficients except the effective elastic coefficient C_{33}^{c}; in that case it provides an overestimated result.

ii. The model based on energy approach provides the results that shows a significant improvement in actuating capabilities of piezoelectric fiber reinforced composite in direction-1 (longitudinal to fiber direction) up to the fiber volume fraction of 0.8. After that the predicted values significantly reduce when compared with the values predicted through strength of materials (SM) and modified strength of materials (MSM) approaches.

iii. The present study also shows that the piezocomposite composed of fibers of piezoelectrically-active materials embedded in piezoelectrically-inactive matrix exhibits superior electric and dielectric properties as compared to monolithic piezoelectric material.

In the second part of the study, the proposed analytical model, viz. modified strength of materials (MSM) has been validated with the finite element method (FEM) based study of the same problem. The effective elastic, piezoelectric and dielectric constants have been estimated as a function of fiber volume fraction in the range of 0.1-0.6 with a step of 0.1. The comparison of results provides an understanding about the effects of fiber packing arrangements and local field fluctuations on the predicted values

of overall properties of piezoelectric fiber reinforced composites. The outcomes of second part of the study or FEM based studies are as follows:

i. The theoretical model proposed in the present work, viz. modified strength of materials (MSM) model shows the predicted value of the overall effective coefficients of the piezoelectric fiber reinforced composite is in more agreement to the calculated values of FEM based approach.
ii. Since, the models based on the conventional strength of materials (SM) approach ignores the effect of fiber packing arrangement while formulation of the model, the proposed model takes in the account the effect of fiber packing arrangement.

The present model is developed assuming loading direction to be transverse to the fiber direction so it is expected to give more precise results for those effective coefficients which are susceptible to the loads given in transverse direction to the fiber orientation which otherwise is not captured in the strength of materials (SM) approach described in the literature. The agreement of the results predicted by the MSM model with those calculated by FEM validates the proposed model. The analytical methods developed in the current study could also serve as a benchmark to study the effective properties of piezoelectric composite involving more complex boundary conditions, e.g., thermo-electro-elastic and magneto-electro-elastic coupling problems.